Electronic Supplementary Material (ESI) for New Journal of Chemistry.

Supporting information for the manuscript

"Coordination vs oxidative rearrangement of photochromic spiropyrans in the reaction with $Fe^{III}Cl_3$ and $Fe^{III}Br_3$"

Nikita N. Osipov,[a] Maxim A. Faraonov,[a] Alexey V. Kuzmin, [b] Salavat S. Khasanov,[b] Alexander F. Shestakov,[a] Tatiana A. Savinykh,[a] Akihiro Otsuka,[d] Hiroshi Kitagawa,[d] and Dmitri V. Konarev*[a]

[a]Federal Research Center of Problems of Chemical Physics and Medicinal Chemistry RAS, Chernogolovka, Moscow region, 142432 Russia; E-mail: konarev3@yandex.ru;

[b]Institute of Solid State Physics RAS, Chernogolovka, Moscow region, 142432 Russia;

[c]Department of Fundamental Physical and Chemical Engineering, M.V. Lomonosov Moscow State University, 119991 Moscow, Russia;

[d] Division of Chemistry, Graduate School of Science, Kyoto University, Sakyo-ku, Kyoto 606-8502, Japan.

Supporting information

Table S1. IR spectra of starting compounds and complexes **1-5**.

Components	TMI-NPS	TMI-NSO	TMI-NPS-$FeCl_3$ (**1**)	TMI-NPS-$FeBr_3$·$2C_6H_4Cl_2$ (**2**)	TMI-NSO-$FeCl_3$·0.5 $C_6H_4Cl_2$ (**3**)	TMI-NSO-$FeBr_3$·0.5 $C_6H_4Cl_2$ (**4**)	$(C_{22}H_{19}N_2O^+)$ $(Fe^{III}Br_4)^-$ (**5**)
Photochromic molecule	456w	406m	478s	478s	-	406w	408w
	-	439w	516m	516m	-	444w	421m
	551w	461m	557m	557m	468w	465w	465m
	589w	471m	571m	571m	-	484m	-
	687w	497m	696m	696m	-	-	493m
	734s	524m	-	-	522w	520w	519m
	745s	551m	-	745s	542m	542m	538m 551w
	753s	560m	760s	760s	565w	560m	-
	808s	576w	802s	802s	575w	574w	-
	820m	594m	822s	822s	607s	607w	607m
	862w	629m	858s	858s	-	-	629w
	936m	646m	928w 952m	928w 952m	641m*	640m*	644w
	987s	692w	972s	972s	697m	699m	697m
	1014m	744s	1018m	1018m	734w	-	730s
	1027m	756s	1036s*	1036s*	758s*	756s^	759s
	1085m	768m	1093s	1094s	-	-	777w
	1108m	820s	1116s	1116s	809s	825s	810s
	1144w	851m	1145s	1144s	-	-	-
	1156m	863m	1159s	1157s	-	872m	878m
	-	890m	1194s	1193s	895w	-	-
	1210w	920w	1213w	1213w	919w	915w	919w
	1238m	930m	1239s	1238s	933m	932w	934s
	1250s	965s	1256m	125	967w	-	965m
	1277m	1006s	1287s	686s	1015s	1019s	1011s
	1304m	1033s	-	5m	1033w*	1032w*	1027w
	1340w	1079 s	1333s	1285s	1089s	1089s	1093m
	1359m	1111s	1361w	-	1105s	-	-
	1379m	1119s	1376s	1331s	-	1114w	1129m
	1441w	1142m	1429m		1134s	1141s	-
	1461m	1152m	1449s*	782m	-	-	1152s
	1488s	1173s	-	1361w	1167m	1166s	1166w
	1516w	1190s	1476s 1503m	1375s	1195s	1191m	1194s
	1590m	1209m	1524s	1429m 1449s*	1215w	1215m	-
	1613m	1244s	1580s	-	1241w	1241s	1231m
	1640m	1250s	-	1476s 1503m	1262s	-	-
	2893w	1274s	-	1524s	1277s	1277s	1272s
	2925w	1303s	2883w	1579s	1319s	1319s	1325s 1342s
	2966m	1359s	2934w	-	1356m	1368m	1367s
	3045m	1384s	2977m	-	1381w	-	-
	3063w	1423s	3057w	2881w	-	-	1408m
		1441m	3074w	2932w	1440s	1440s	1439s
		1459s		2976m	1453m*	1461m*	1456s
		1484s		3058w	1490w	1476m 1490s	1473w
		1510s		3072w	1518m	1510w	1518s
		1569m			1556m	1550m	-
		1592s			1569s	1588m	1568s
		1609s			1604s	1614m	1599s
		1622s			-	-	1624m
		2815m			2814w	2851w	2851w
		2872m			2892w	-	
		2889m			-	-	
		2923m			2917w	2921m	2931w
		2964s			2964w	2956w	2976w
		3027w					-
		3066w					3076w
$C_6H_4Cl_2$				640s	641m*	640m*	
				760s	758s*	756s*	
				1036s*	1033w*	1032w*	
				1448s*	1453m*	1461m*	

Abbreviation: w: weak, m: middle, s- strong intensity, sp. – split band, *: bands are overlapped

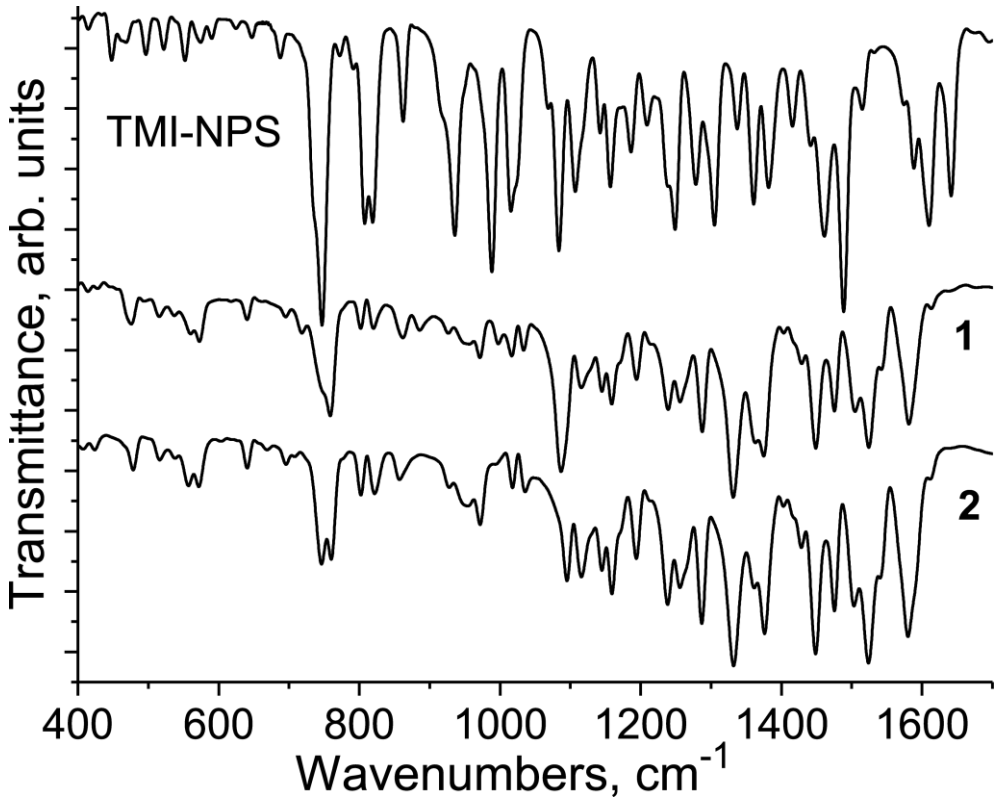

Fig. S1. IR spectra of starting TMI-NPS and coordination complexes TMI-NPS-$FeCl_3$ (**1**) and TMI-NPS-$FeBr_3 \cdot 2C_6H_4Cl_2$ (**2**) in KBr pellets prepared in anaerobic conditions.

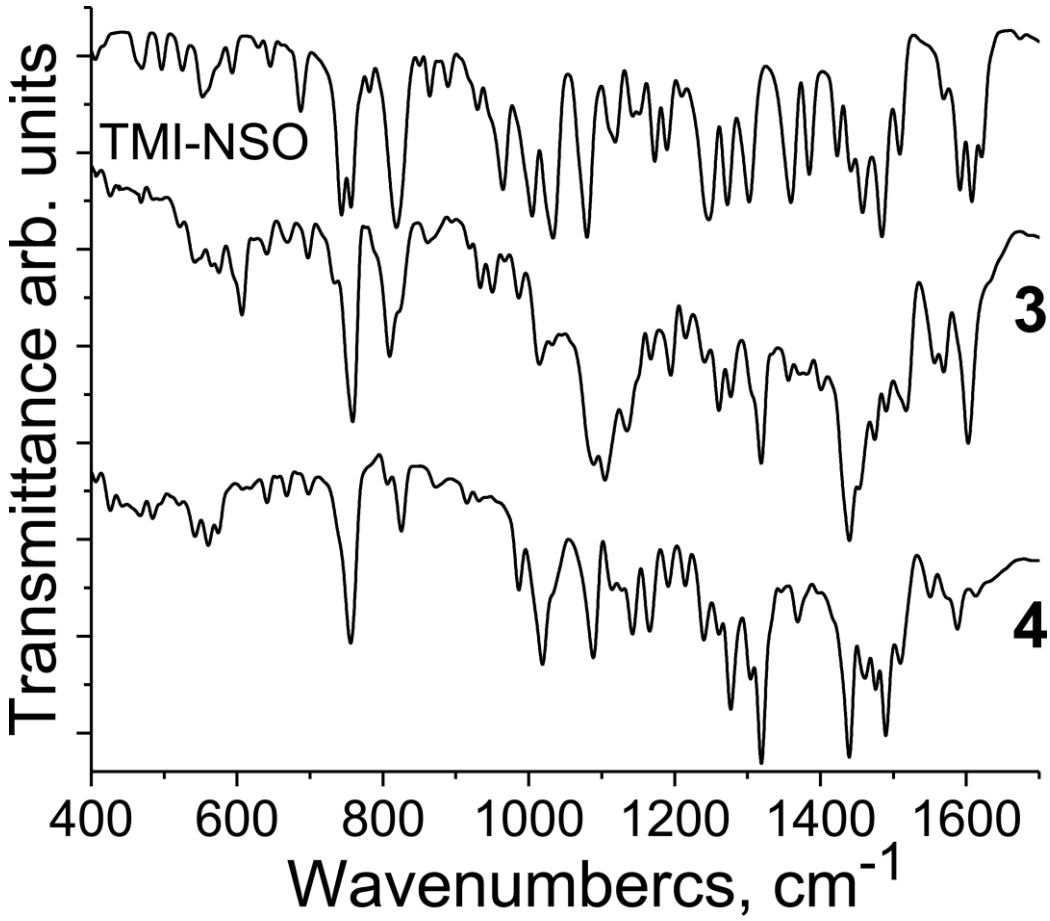

Fig. S2. IR spectra of starting TMI-NSO and coordination complexes TMI-NSO-$FeCl_3 \cdot 0.5C_6H_4Cl_2$ (**3**) and TMI-NSO-$FeBr_3 \cdot 0.5C_6H_4Cl_2$ (**4**) in KBr pellets prepared in anaerobic conditions.

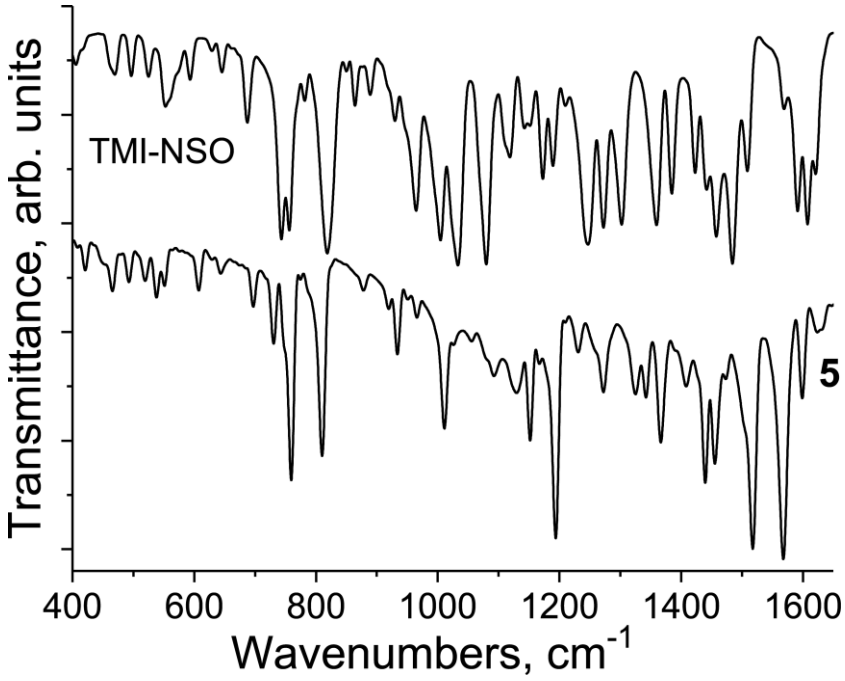

Fig. S3. IR spectra of starting TMI-NSO and product obtained via the oxidation of this photochromic molecule by $Fe^{III}Br_3$ in the presence of HATNA in KBr pellets.

Crystal structures of complexes 1 and 5

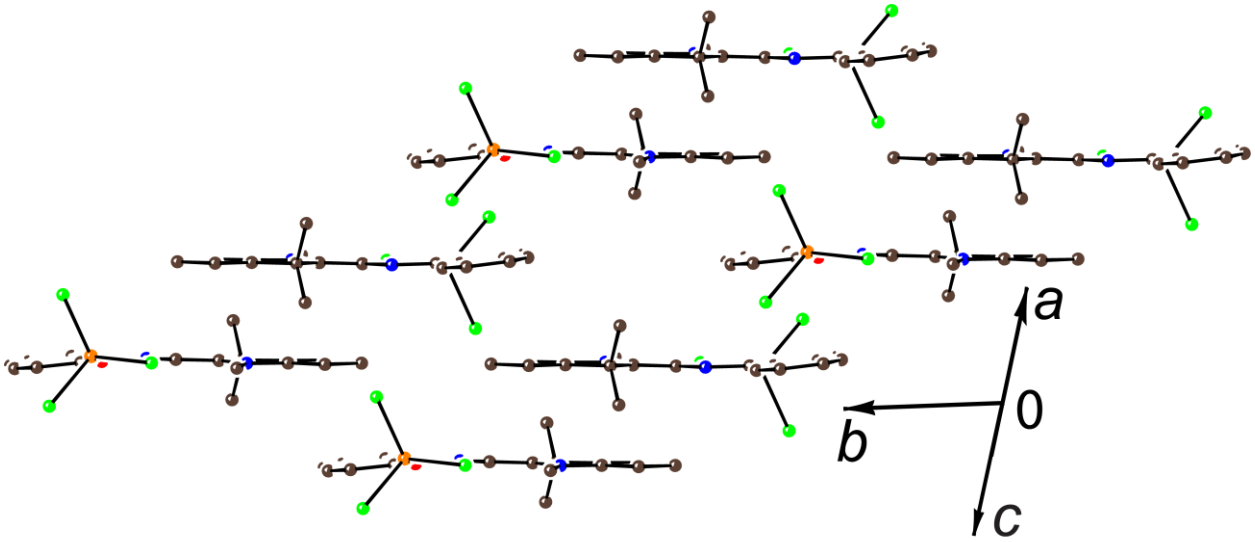

Fig. S4. View on the packing of TMI-NPS-$FeCl_3$ molecules in **1**.

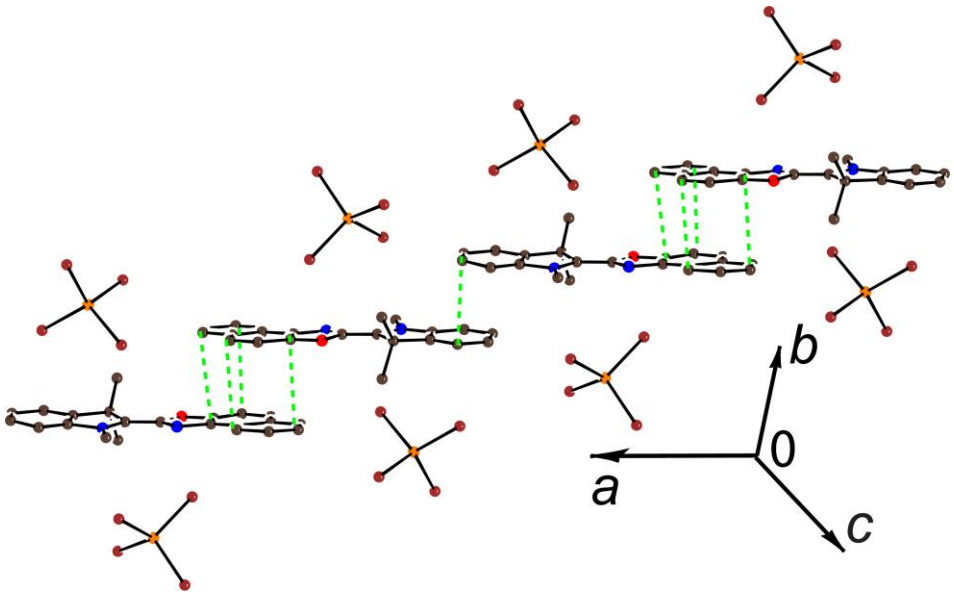

Fig. S5. View on the packing of the ($C_{22}H_{20}N_2O^+$) and $Fe^{III}Br_4^-$ ions in **5**. Short van der Waals C…C contacts between cations are shown by green dashed lines.

Data of magnetic measurements for complexes 1-5
Complex 1

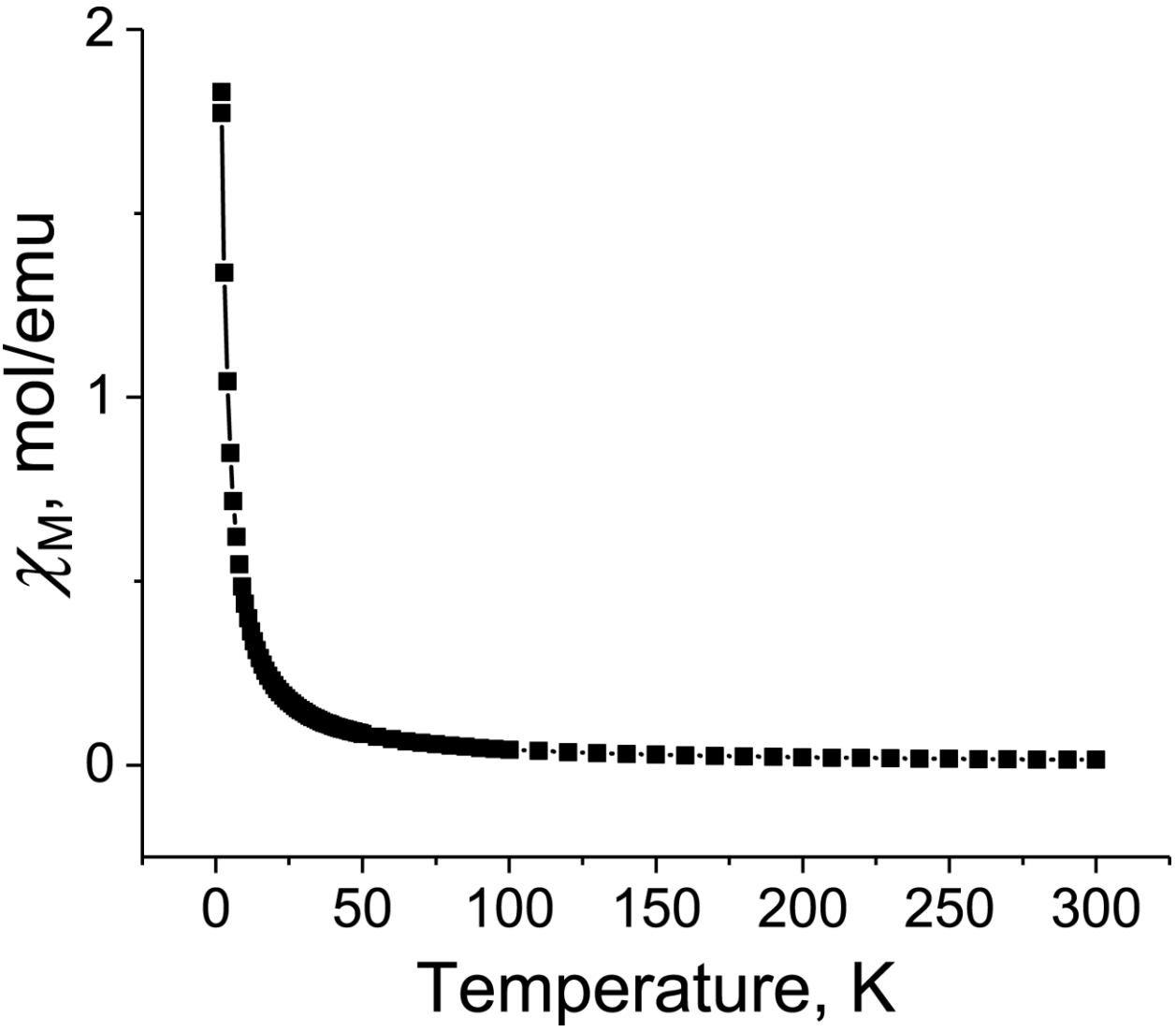

Fig. S6. Temperature dependence of molar magnetic susceptibility for polycrystalline **1** in the 1.9-300 K range after the subtraction of a temperature independent contribution.

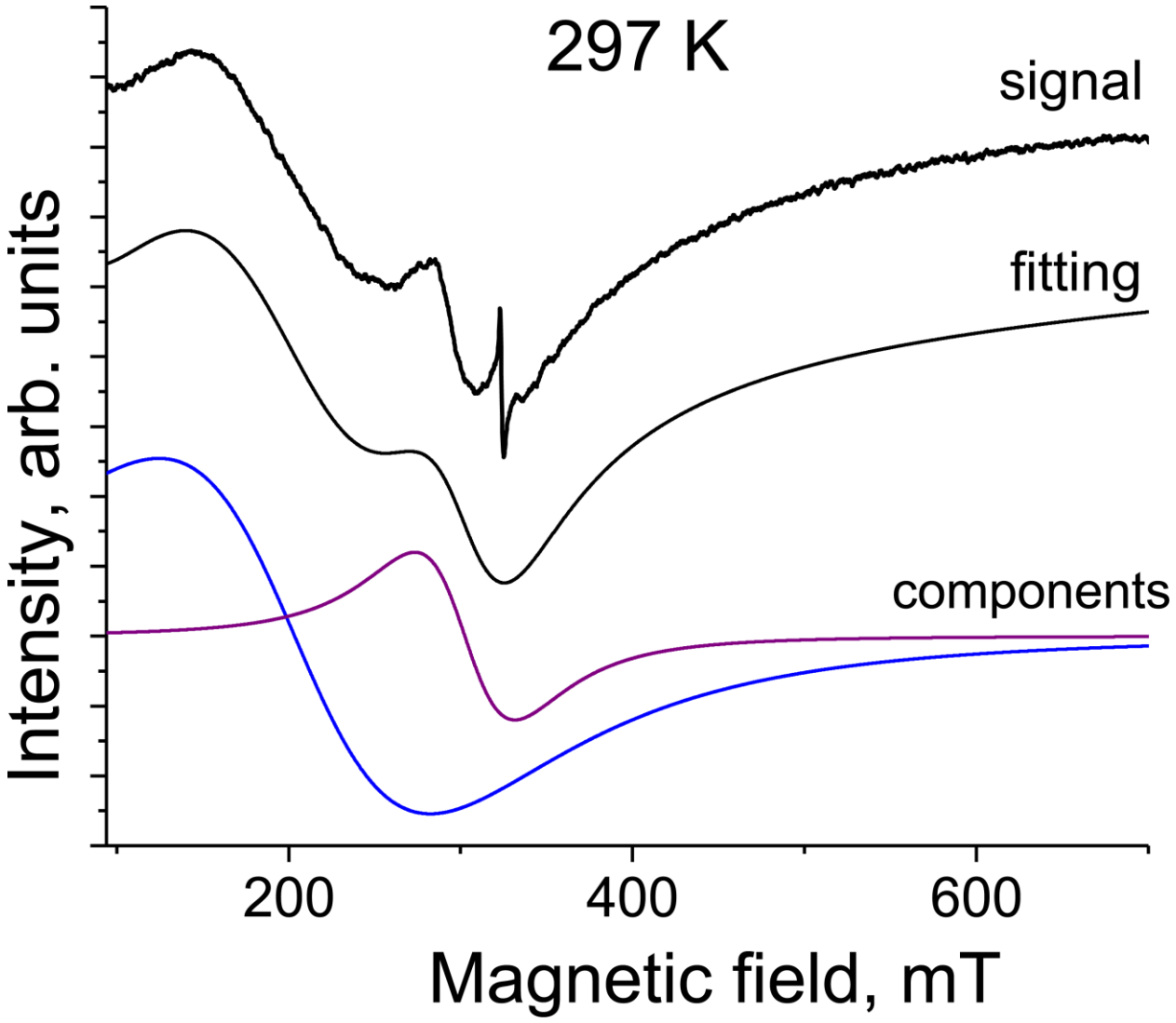

Fig. S7. EPR spectrum of polycrystalline **1** at 297 K. Fitting of the signal by two Lorentzian lines is shown below. Fitting of a narrow line at g = 2.008 is not shown.

Complex 2

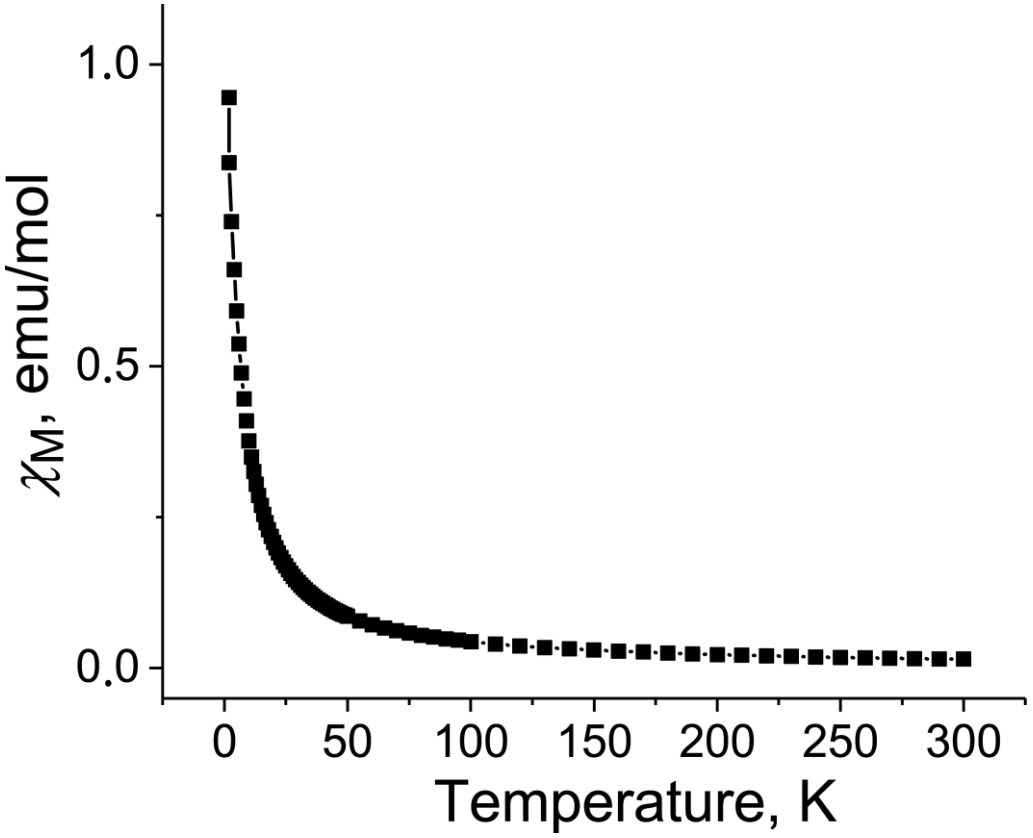

Fig. S8. Temperature dependence of molar magnetic susceptibility for polycrystalline **2** in the 1.9-300 K range after the subtraction of temperature independent contribution. .

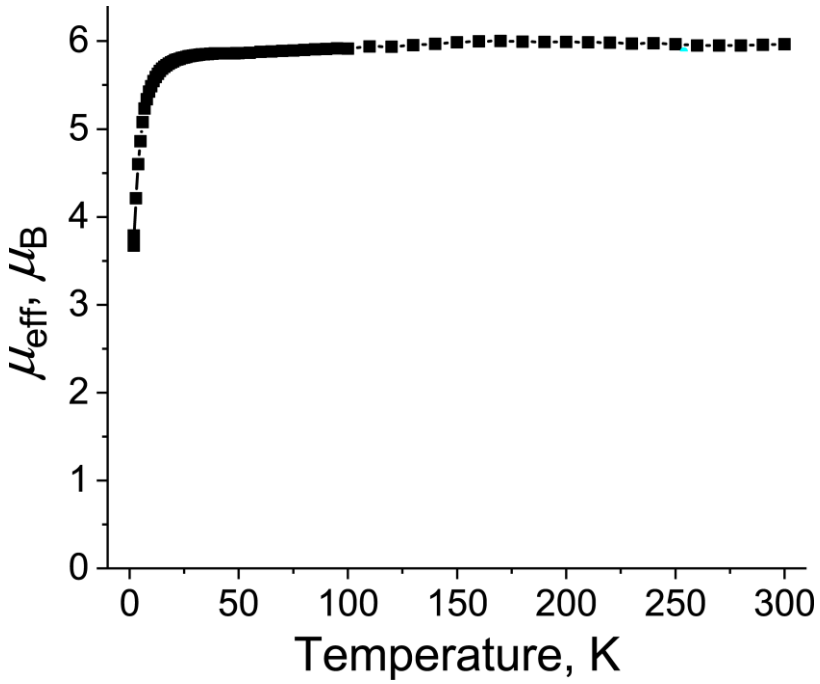

Fig. S8. Temperature dependence of effective magnetic moment for polycrystalline **2** in the 1.9-300 K range.

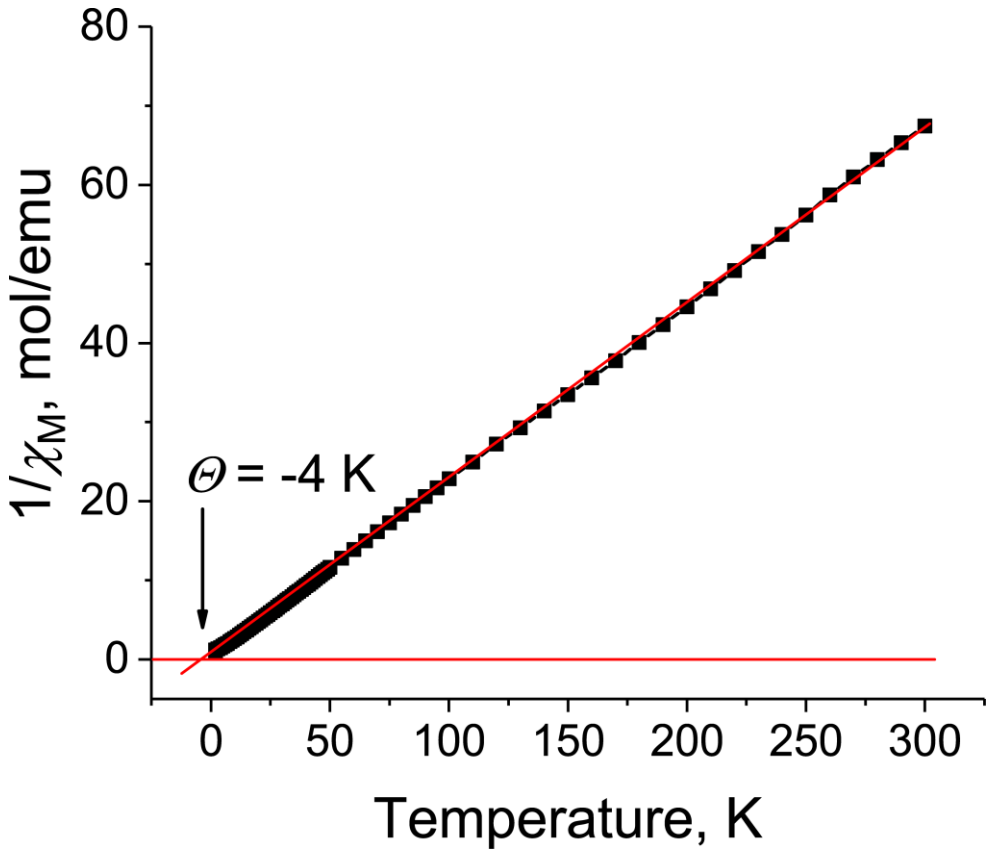

Fig. S9. Temperature dependencies of reciprocal molar magnetic susceptibility for polycrystalline **2** in the 1.9-300 K range.

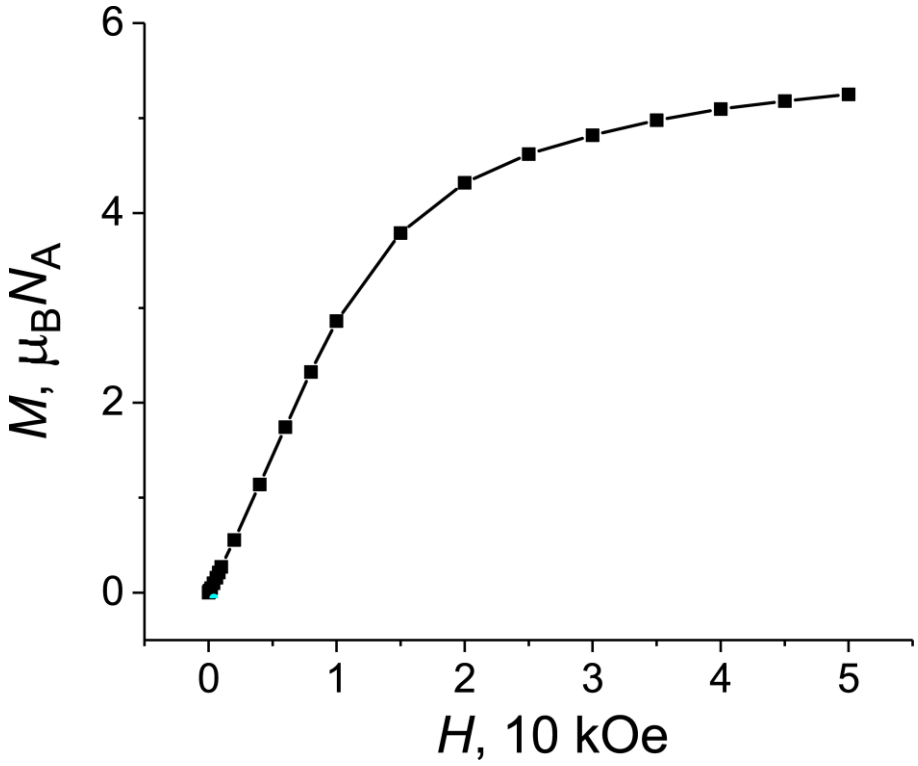

Fig. S10. Dependence of magnetization *vs* magnetic field up to 50 kOe for polycrystalline **2**.

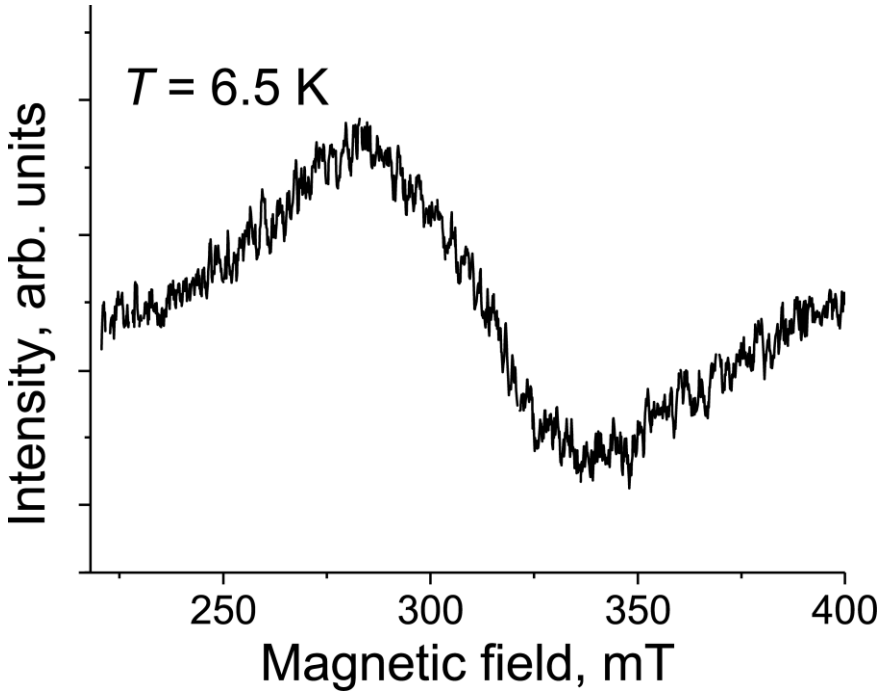

Fig. S11. Temperature dependence for polycrystalline **2** at 6.5 K. Signal can be fitted by one Lorentzian line, parameters of fitting are shown in Table 4.

Complex 3

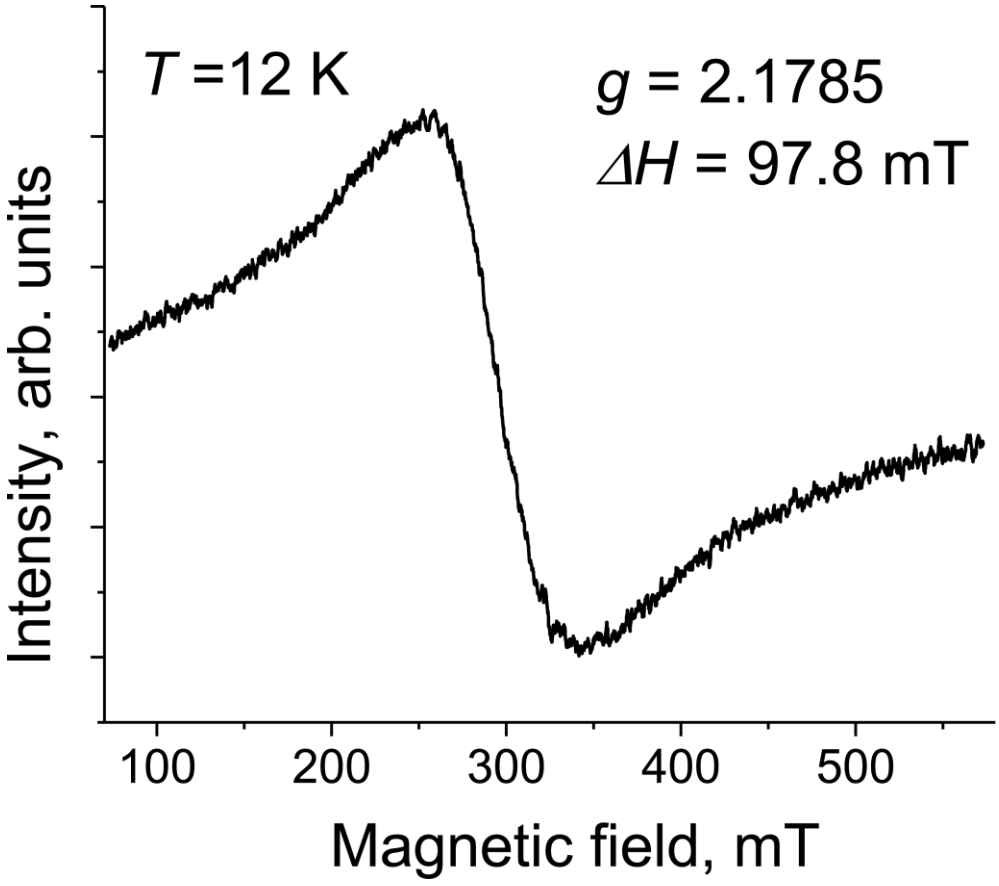

Fig. S12. EPR spectrum of polycrystalline **3** at 12 K.

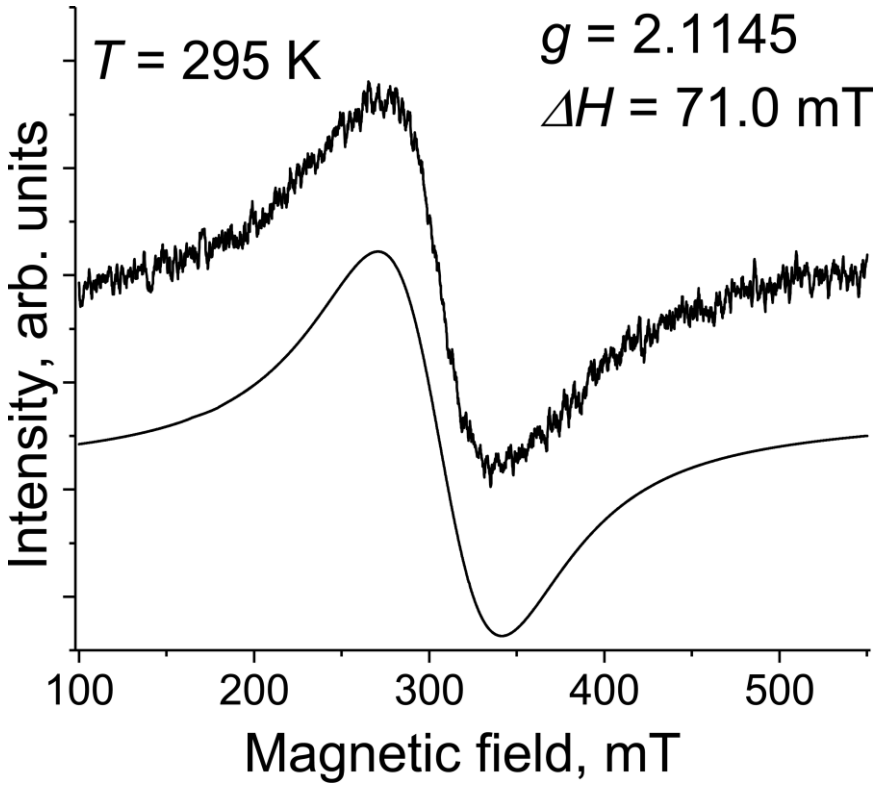

Fig. S13. EPR spectrum of polycrystalline **3** at 295 K. Fitting of the signal by one Lorentzian line is shown below.

Complex 4

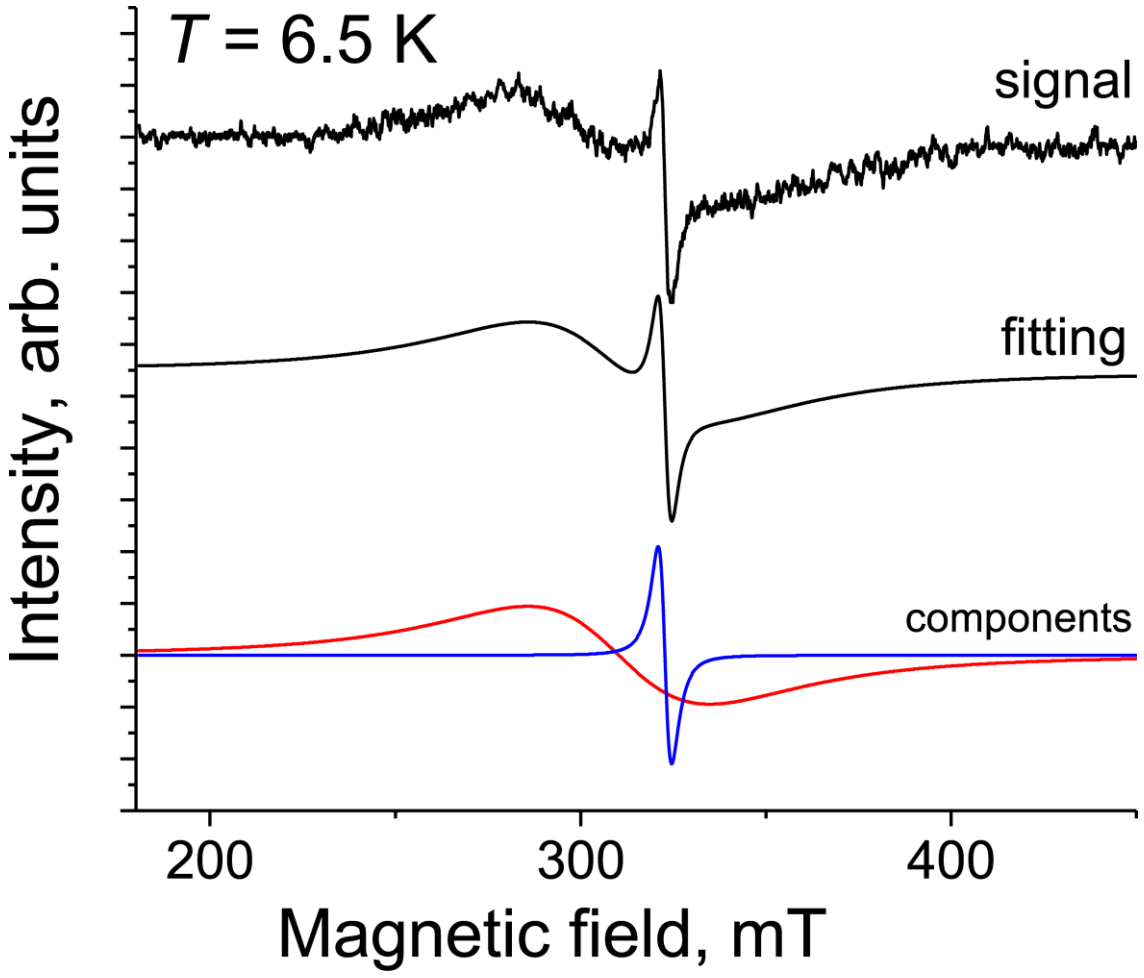

Fig. S14. Temperature dependence for polycrystalline **4** at 6.5 K. Signal can be fitted by two Lorentzian lines, parameters of fitting are shown in Table 4.

Salt 5

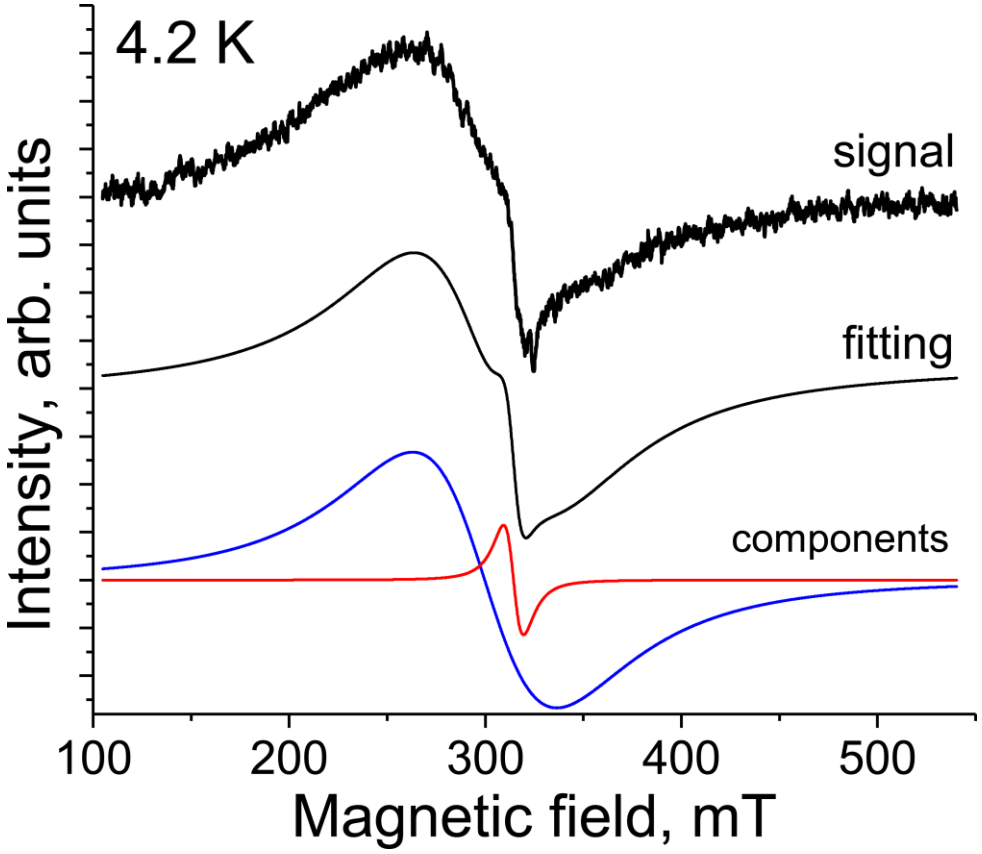

Fig. S15. Temperature dependence for polycrystalline **5** at 4.2 K. Signal can be fitted by two Lorentzian lines, parameters of fitting are shown in Table 4.

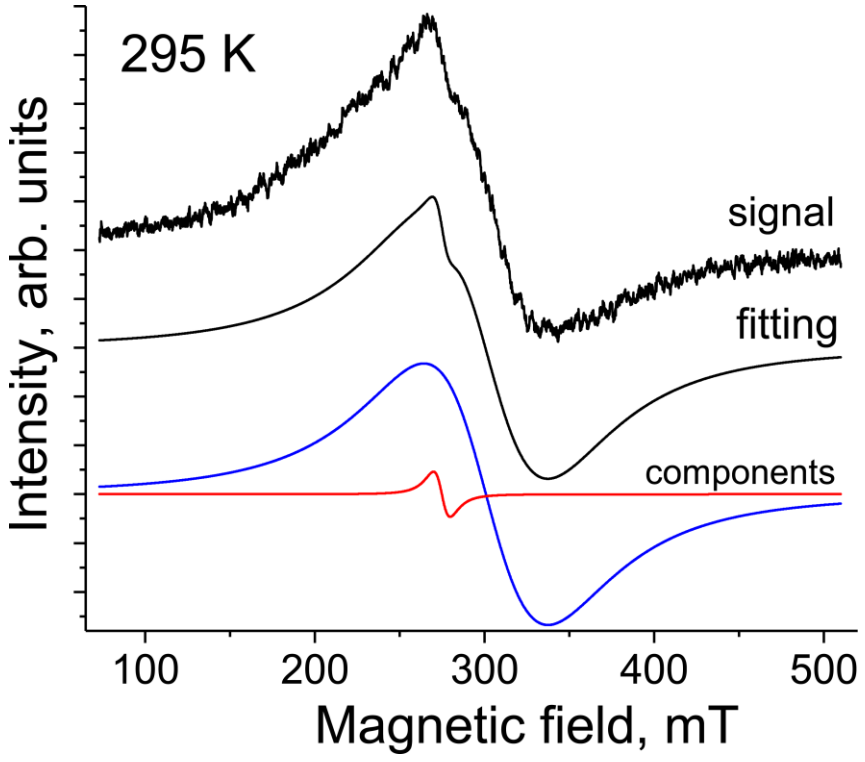

Fig. S16. Temperature dependence for polycrystalline **5** at 295 K. Signal can be fitted by two Lorentzian lines, parameters of fitting are shown in Table 4.

Theoretical part

The molecular structures were optimized using the PBE exchange-correlation functional [1] and with the extended basis set Fe: [9s9p8d/5s5p4d], Cl, Br [5s5p2d/3s3p2d], N,C :[5s5p2d/3s3p2d], H:[5s1p/3s1p] for the valence electrons and the SBK pseudopotential[2] implemented in the PRIRODA package [3]. The Hirschfeld method [4] was used to calculate atomic charges. Electronic spectra were calculated using transition energies and oscillator strengths found by TDDFT and fixed linewidth of 1600 cm^{-1} for the Gaussian peaks. All calculations were performed at Joint Supercomputer Center of the Russian Academy of Sciences.

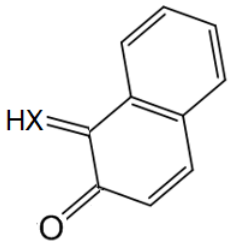

Fig. S17. Naphthalene analogs of spiropyrans discussed in the text.

The reason for the increase in dipole moment of TMI-NPS and TMI-NSO molecules in the open form from 1 Debye to 4.4 and 5.1 Debye, respectively, is the appearance of a polar carbonyl group in the open form of spiropyrans. Indeed, naphthalene moieties related to TMI-NPS and TMI-NSO (only half of open spiropyran, Fig. S17) have a similar dipole moment of 4.0 or 4.5 Debye, respectively, but with a shorter C-O bond length by 0.02 Å in the carbonyl group.

Nevertheless, the possibility of the transition to the zwitterionic form is manifested in the formation of coordination complexes. The estimated energy for the addition of TMI-NSO and TMI-NPS in the open form to $Fe^{III}Br_3$ and $Fe^{III}Cl_3$ is 33.7 and 36.0 kcal/mol and 35.2 and 37.5 kcal/mol, respectively.

For comparison, the coordination of $Fe^{III}Br_3$ to the carbonyl group of naphthalene analogs of TMI-NSO and TMI-NPS (Fig. S17) gives a noticeably smaller energy gain of 21.3 and 25.0 kcal/mol. In this case, an increase in dipole moment to 10.6 and 11.8 Debye, respectively, is observed due to donor-acceptor electron density transfer from the organic ligand to the Fe^{III} center, 0.30 and 0.32 e, respectively.

This transfer is stronger by 0.09 e in the $Fe^{III}Br_3$ complexes with TMI-NSO and TMI-NPS due to an additional contribution of the zwitterionic form. That increases dipole moment to 13.2 and 14.2 Debye and provides more pronounced elongation of the C-O bond by 0.045 Å. Total energy gain in these complex formation reactions is:

2TMI-NPS + $Fe^{III}{}_2X_6$ = 2 **(**TMI-NPS·$Fe^{III}X_3$) + 38.6 (X = Br); 42.6 (X=Cl) kcal/mol.

2TMI-NSO + $Fe^{III}{}_2X_6$ = 2(TMI-NSO·$Fe^{III}X_3$) + 38.3 (X = Br); 42.2 (X = Cl) kcal/mol.

The presence of some amount of open forms of the TMI-NPS and TMI-NSO is also expected in the equilibrium. That facilitates the formation of these complexes. Tables S2 and S3 show geometric parameters of the ligands in the open form when they form complexes with $Fe^{III}X_3$.

Table S2. Calculated geometric parameters of $Fe^{III}X_3$ complexes with the open form of TMI-NPS.

Coordination unit	N–C, Å 1	C–C, Å 2	C–C(N), Å 3	C(N)–C, Å 4	C–C, Å 5	C–O, Å 6	Fe-O, Å	Fe-X, Å	contact O…H, Å
Free ligand	1.380	1.387	1.412	1.399	1.490	1.254			2.002
$Fe^{III}Cl_3$*	1.362	1.402	1.396	1.419	1.450	1.298	1.929	2.223 2.205 2.223	2.037
$Fe^{III}Cl_3$	1.363	1.402	1.398	1.416	1.452	1.299	1.955	2.224 2.206 2.206	2.075
$Fe^{III}Br_3$*	1.362	1.403	1.395	1.418	1.450	1.298	1.928	2.368 2.348 2.367	2.057
$Fe^{III}Br_3$	1.363	1.403	1.398	1.415	1.452	1.299	1.955	2.367 2.350 2.350	2.096

*rotation isomer of the complex in which $Fe^{III}X_3$ fragment is rotated about the Fe-O bond by 180°
Numbers are given according to Fig. 1 in the main text.

Table S3. Calculated geometric parameters of $Fe^{III}X_3$ complexes with the open form of TMI-NSO**.**

Coordinati unit	N–C, Å 1	C–C, Å 2	C–C(N), Å 3	C(N)–C, Å 4	C–C, Å 5	C–O, Å 6	Fe-O, Å	Fe-X, Å	contact O…H, Å
Free ligand	1.373	1.394	1.349	1.331	1.498	1.252			2.015
$Fe^{III}Cl_3$*	1.357	1.410	1.329	1.350	1.461	1.294	1.937	2.216 2.225 2.203	2.011
$Fe^{III}Cl_3$	1.358	1.412	1.330	1.348	1.460	1.295	1.955	2.227 2.203 2.203	2.033
$Fe^{III}Br_3$*	1.356	1.411	1.329	1.350	1.460	1.294	1.933	2.364 2.366 2.344	2.027
$FeBr_3$	1.357	1.411	1.331	1.346	1.462	1.295	1.959	2.367 2.347 2.346	2.058
$Fe^{III}Br_3$**	1.357	1.415	1.328	1.351	1.451	1.340	1.888	2.378 2.352 2.352	2.039
$Fe^{III}Br_3$[#]	1.356 1.356	1.416 1.416	1.327 1.326	1.351 1.351	1.456 1.456	1.300 1.300	1.943 1.942	2.369 2.360 2.345 2.369 2.361 2.345	2.081 2.078
$FeBr_4^{-}$[&]	1.339	1.423	1.323	1.366	1.409	1.362		2.388 2.340 2.389 2.398	

*rotation isomer of the complex in which $Fe^{III}X_3$ fragment is rotated about the Fe-O bond by 180°
Numbers are given according to Fig. 1 in the main text.
**complex with fixed Fe-O and C-O bonds.
[#] dimer complex (TMI-NSO·$Fe^{III}Br_3$)$_2$
[&] complex [($C_{22}H_{19}N_2O^+$)($FeBr_4^-$)].

It is clear from Tables S2 and S3 that the structure of spiropyrans is similar in the complexes with $Fe^{III}Cl_3$ and $Fe^{III}Br_3$. The main discrepancy with experimental data is observed for the lengths of Fe-O and O-C bonds. However, calculations for the rotational isomers show that these bond lengths vary even for different orientations of the $Fe^{III}X_3$ fragment (rotation by 180° about the Fe-O axis). Therefore, the Fe-O bonds are very labile. Moreover, fixing the lengths of Fe-O and O-C bonds as a length of the bonds experimentally determined from X-ray diffraction (line $FeBr_3$**) has a weak effect on geometry of the organic ligand and requires very small energy costs of about 2 kcal/mol, comparable with the energy of intermolecular interaction. For example, the formation of a $(TMI\text{-}NSO\cdot Fe^{III}X_3)_2$ dimer is accompanied by a decrease in energy by 6.9 kcal/mol. In this dimer, similar changes in geometry of the organic ligand occur when the values of the Fe-O and O-C bond lengths are fixed.

The energy diagram of transformations of the skeleton of the isolated $TMI\text{-}NSO^{\bullet+}$ radical cation is shown in Fig. S18, and the molecular structures for the intermediate and transition states are shown in Figs. S19 and S20.

The $TMI\text{-}NSO^{\bullet+}$ radical cation (Fig. S19, str. I) appears as a result of intramolecular electron transfer in the $[TMI\text{-}NSO\cdot(Fe^{III}Br_3)_2]$ adduct. The cleavage of the O=C bond in its six-membered ring and the subsequent formation of a new O-CH bond in the five-membered (oxazole) ring (Fig. S19, str. III) proceeds via the intermediate open form (Fig. S19, str. II) of the $TMI\text{-}NSO^{\bullet+}$ radical cation with a small gain in energy and minor energy barriers. This intermediate product is unstable with respect to intramolecular migration of the H atom (1-2 shift) to neighboring nitrogen or carbon atoms, but it is hardly possible since this migration requires overcoming a noticeable energy barrier. The corresponding structures for the final and transition states are shown in Figs. S19 and S20.

For the formed intermediate with an oxazole ring (Fig. S19, str. III), abstraction of the H atom from the quaternary carbon atom requires very low energy of 24.6 kcal/mol only since that provides the formation of a double C=N bond and is comparable with the affinity of the $Fe_2Br_6^-$

anion to the H atom, which achieves 29.8 kcal/mol. That makes it possible to form a $TMNOY^+$ cation as a result of intermolecular H atom transfer in the isomer form of [TMI-NSO·$(Fe^{III}Br_3)_2$] adduct with oxazole ring. Analysis of the energy profile of the [TMI-NSO·$(Fe^{III}Br_3)_2$] adduct transformation confirms this conclusion.

To study this process, we used the total spin of the system equal to 4, which arises at the antiparallel orientation of the spins of the metal complex $S = 9/2$ and the radical cation $S = 1/2$ and coincides with the spin of the intermediate product [$(TMNOY^+)$ $(HFe_2Br_6)^-$] after the transfer of the H atom from TMI-$NSO^{\bullet+}$ to the $(Fe^{III}Br_3)_2$ dimer. The total energy released in this reaction is positive:

$(TMI\text{-}NSO^{\bullet+})(Fe_2Br_6^-)$ = [$(TMNOY^+)$ $(HFe_2Br_6^-)$] + 2.0 kcal/mol

The first stage of adduct formation with charge transfer occurs with a slight decrease in energy of 1.4 kcal/mol. However, because of the loss of entropy due to a decrease in number of particles in this reaction, the corresponding equilibrium constants will be noticeably less than a unit. Therefore, the presence of HATNA in the system is of great importance for irreversibility of the second oxidation and deprotonation processes. The HBr molecule is weakly bound in the complex ($HFe_2Br_6^-$), and its transfer to the HATNA base is accompanied by a noticeable gain in energy.

$(HFe_2Br_6^-)$ + HATNA = (Fe_2Br_5) + HATNA(HBr) +7.5 kcal/mol

In addition, the replacement of a binuclear anion by a more compact mononuclear anion also gives an energy gain.

[$(TMNOY^+)(HFe_2Br_6^-)$] + $(FeBr_4^-)$ = [$(TMNOY^+)(FeBr_4^-)$] + $(HFe_2Br_6^-)$ + 3.7 kcal/mol

The entropy of the system changes little in these reactions, and, as a result, the equilibrium is strongly shifted towards the observed product [$(TMNOY^+)(FeBr_4^-)$].

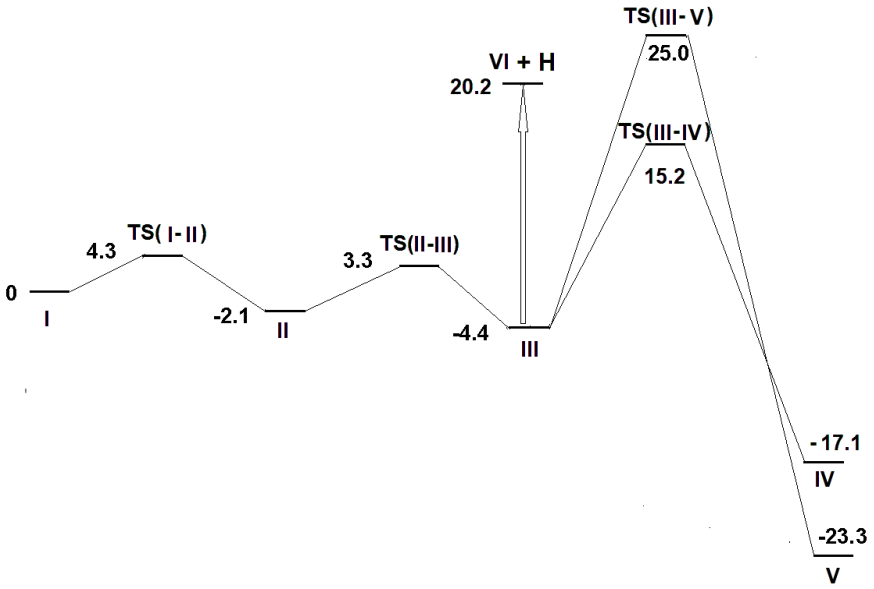

Fig. S18. Energetic scheme of transformations of the TMI-NSO$^{\bullet+}$ radical cation. Intermediate states are marked from I to V, and transition states are from TSI-III to TS III-V. Molecular structures for these states are shown in Figs. S19 and S20.

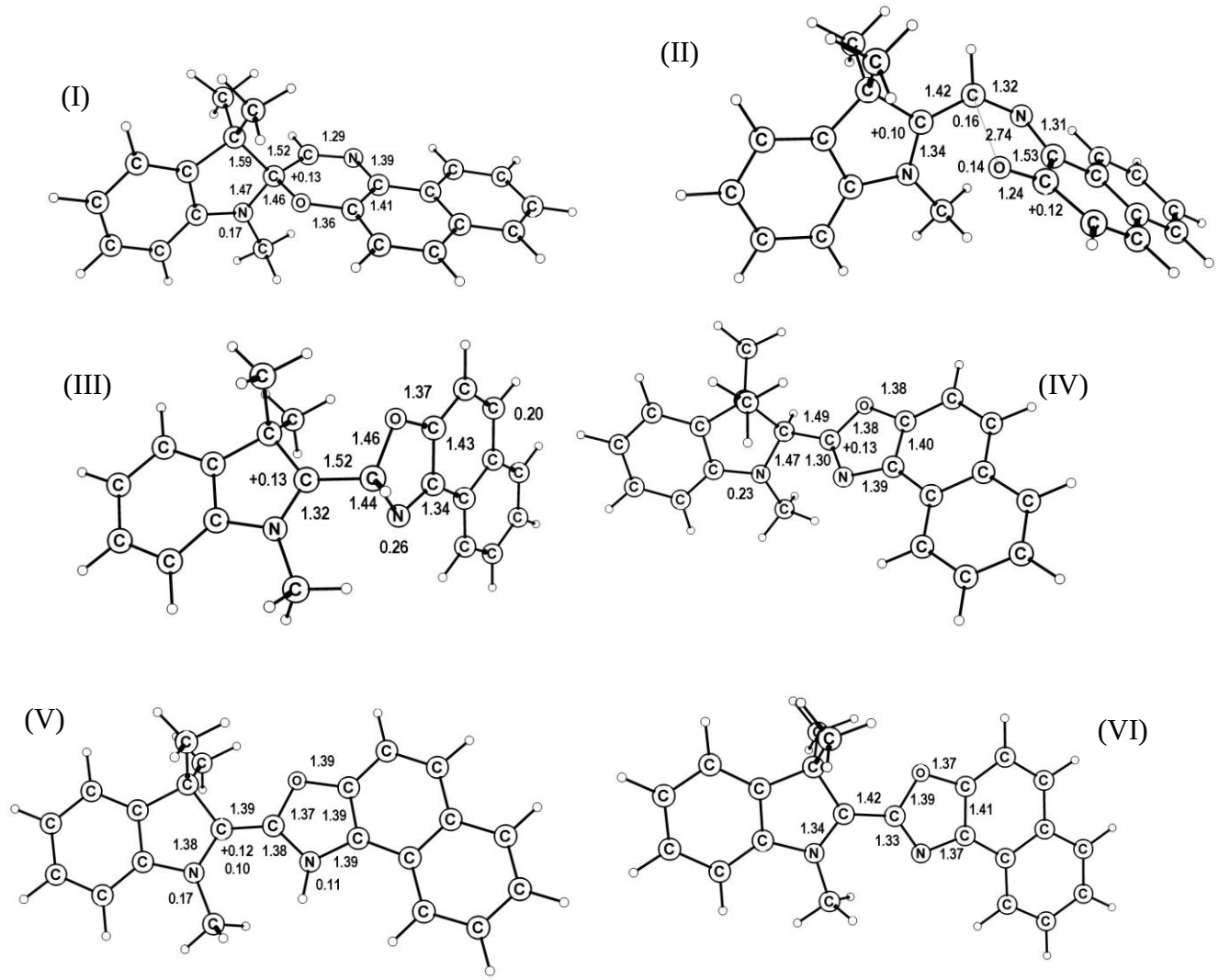

Fig. S19. Molecular structure of the TMI-NSO$^{\bullet+}$ radical cation (I) and the products of its transformations. The lengths of the main bonds are given together with the values of maximal localization of positive charge (marked by +), and spin density is placed near the corresponding atoms.

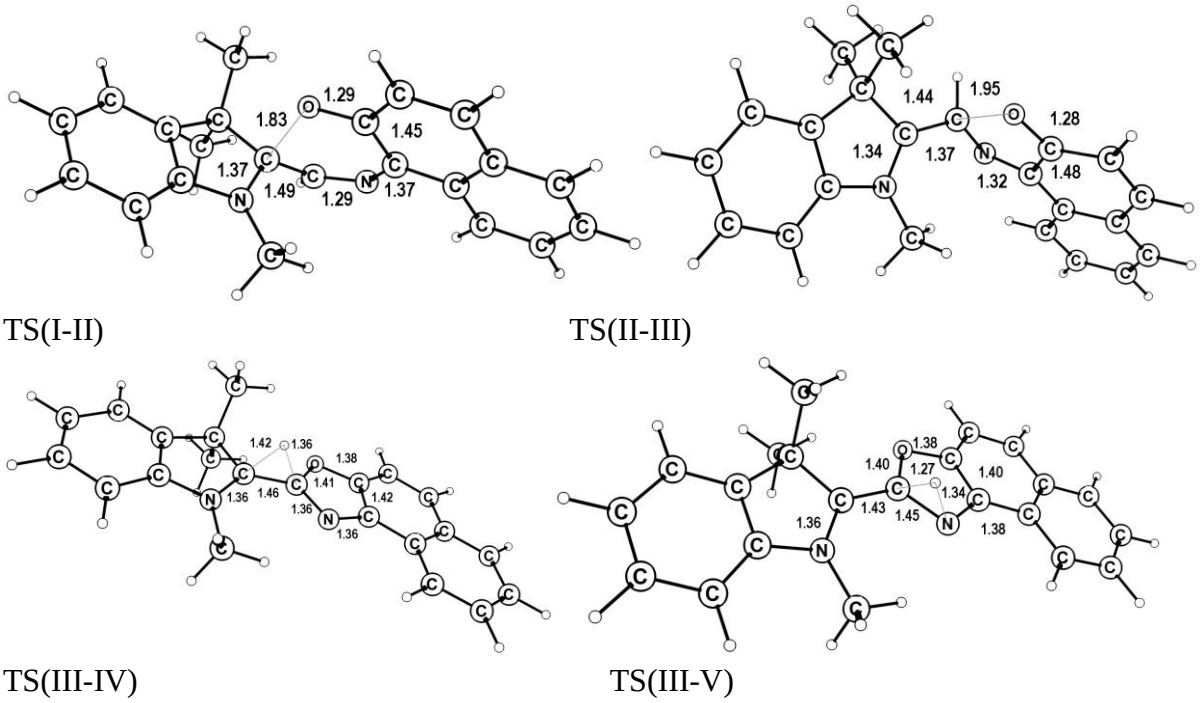

Fig. S20. Molecular structure of the transition states of the TMI-NSO$^{\bullet+}$ radical cation transformations.

The energy profile of the transformation of the low-spin adduct [(TMI-NSO^{+})($Fe_2Br_6^{-}$)] is shown in Fig. S21.

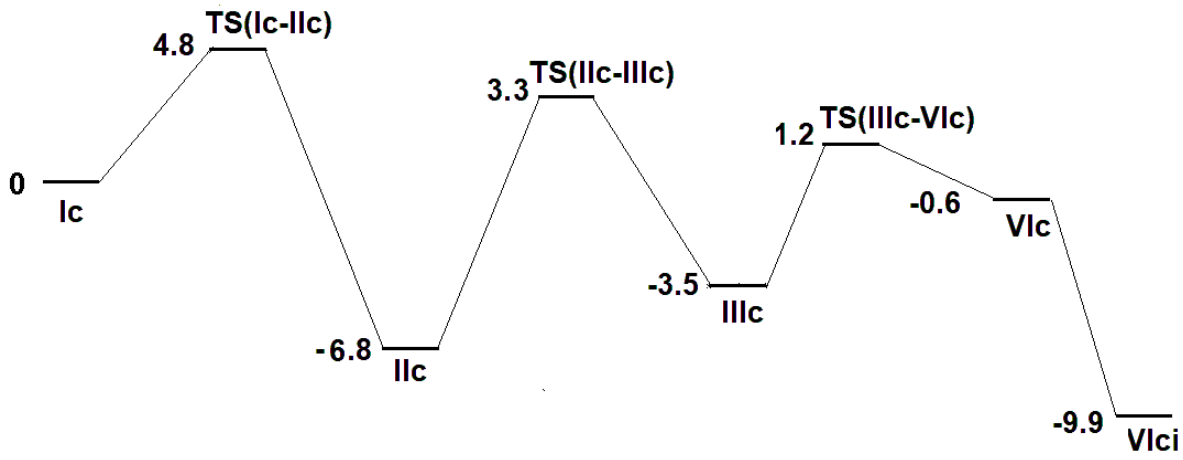

Fig S21. Energetic scheme of transformations of the adduct of TMI-NSO and the Fe_2Br_6 dimer.

The structure of transition and intermediate states are shown in Figs. S22 and S23.

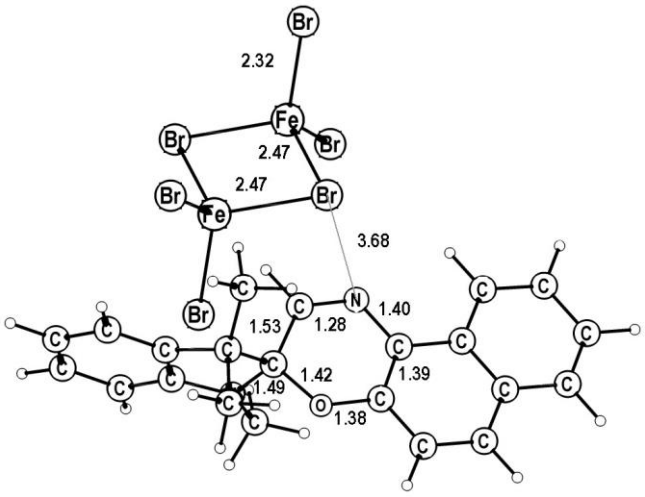

(Ic)

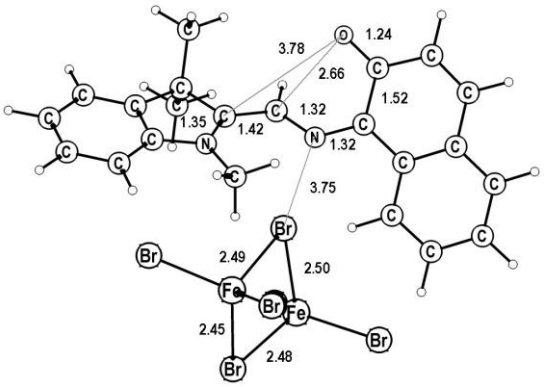

(IIc)

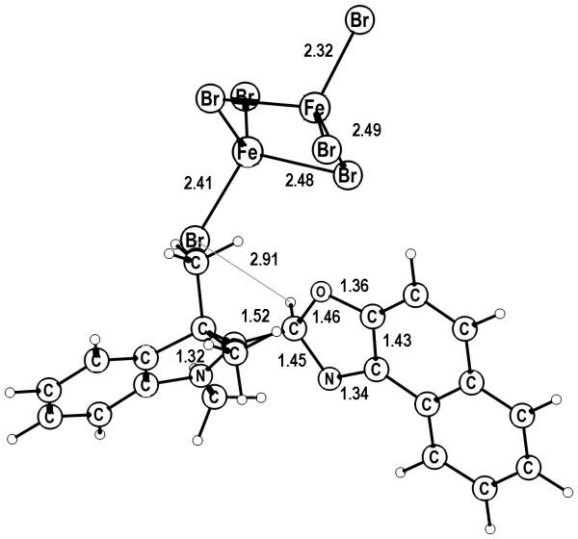

(IIIc)

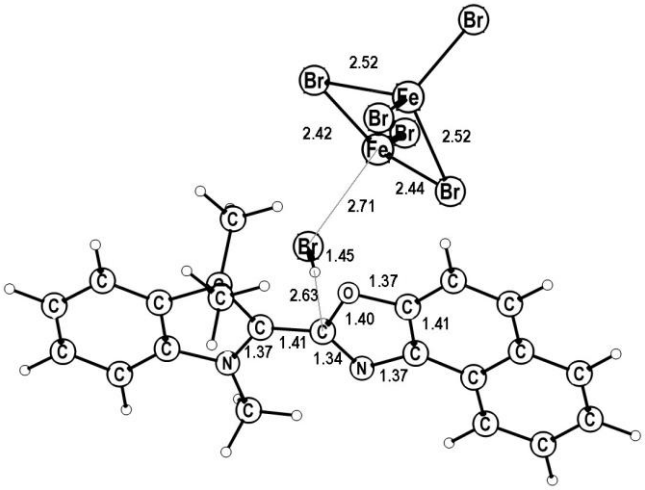

(VIc)

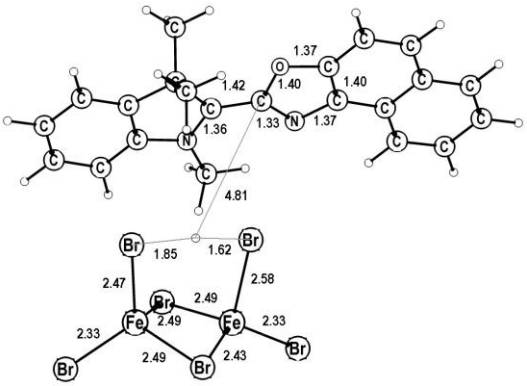

(VIci)

Fig. S22. Molecular structure of the [(TMI-NSO$^{\bullet+}$)($Fe_2Br_6^-$)] adduct (Ic) in low-spin state and the products of its transformations.

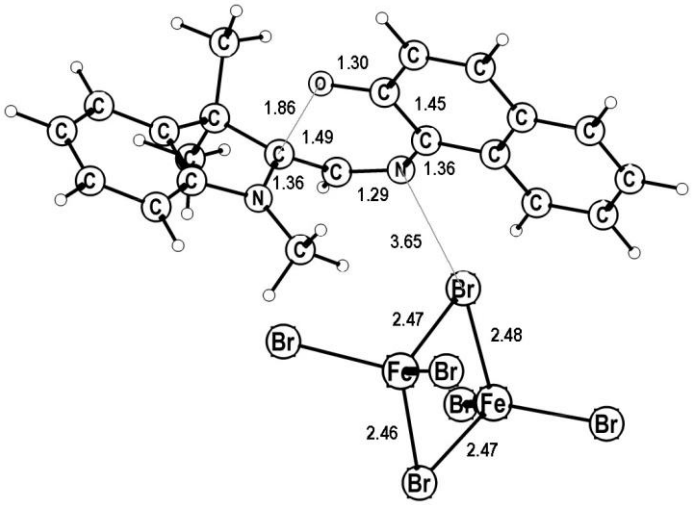

TS(Ic- IIc)

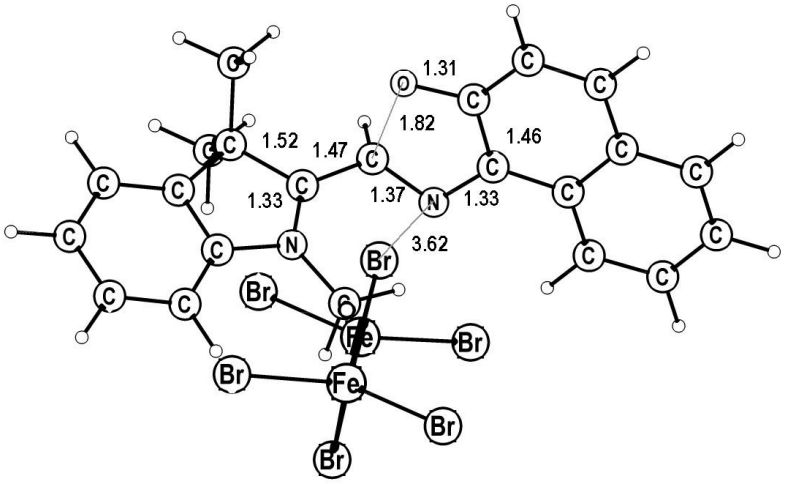

TS(IIc- IIIc)

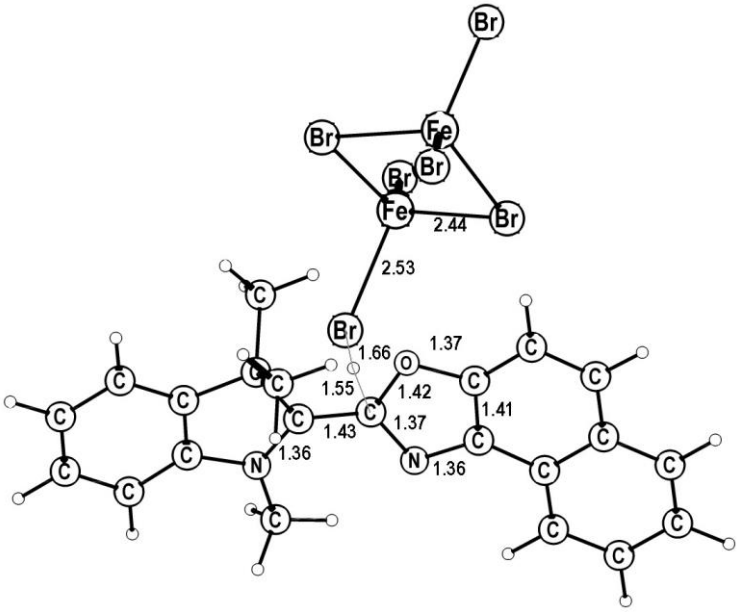

(TS(IIIc-VIc)

Fig. S23. Molecular structure of the transition states of the transformations of low-spin state adduct [(TMI-NSO$^{\bullet+}$)($Fe_2Br_6^-$)].

The initial stages of the formation of the open form of the radical cation in the complex and its transformation to the isomeric closed form have insignificant energy barriers. The final stage of transfer of the H atom to the iron complex also has low activation energy and is accompanied by a slight increase in energy. At this stage, [(TMNOY^{+})(HFe_2Br_6)$^{-}$] with a weakly bound HBr molecule in the anionic part is obtained. There are two strong intramolecular hydrogen bonds with hydrogen atoms in the main isomer of the ($HFe_2Br_6^{-}$) complex. As a result, the VIc-VIci transition noticeably decreases in energy. However, no direct formation of this isomer from intermediate complex IIIc was found.

The initial adduct [(TMI-NSO$^{\bullet+}$)($Fe_2Br_6^{-}$)] in the high-spin state has energy 6.1 kcal/mol lower than the low-spin state and has a lower dipole moment of 10.8 Debye due to admixture of a state with no charge transfer. However, the activation energy of 5.8 kcal/mol required for its transition to the open form is almost the same as for a low-spin system. In the open form, the high-spin complex has a higher dipole moment of 11.8 Debye than the original adduct. Its energy is 2.7 kcal/mol lower than the energy of the low-spin complex in its open form. The next high-spin intermediate IIIc has a dipole moment of 19.7 Debye, which is similar to that for the low-spin one, and their energies are also almost equal. However, further transfer of a hydrogen atom is possible only for a low-spin system since the binuclear ($HFe_2Br_6^{-}$) complex should have a spin of 4 in the ground state. High energy is required to unpair two electrons from the Fe-Br bonding orbitals to get spin of 5. Thus, there is a fairly smooth energy profile with small barriers to the transformation of the initial adduct [(TMI-NSO$^{\bullet+}$)($Fe_2Br_6^{-}$)] to the intermediate [(TMNOY^{+})($HFe_2Br_6^{-}$)] complex.

Optical spectra

Calculated spectra of the **(**TMI-NPS·$Fe^{III}X_3$) and (TMI-NSO·$Fe^{III}X_3$) complexes and the spectra of spiripyrans in the open forms are shown in Figs. S24 and S25. In general, the calculated spectra of the $Fe^{III}Cl_3$ and $Fe^{III}Br_3$ complexes are quite close to each other in terms of positions

and intensities of absorption bands. This correspondence is realized for the observed spectra of the (TMI-NSO·$Fe^{III}X_3$) complexes. In the case of the TMI-NPS ligand, the experimental spectra (Fig. 3, compounds 1 and 2) show an increase in the intensity of the 822 nm band for the $Fe^{III}Br_3$ complex as compared with the intensity of the 844 nm band for the $Fe^{III}Cl_3$ complex. Since the experimental spectra refer to condensed phase, this discrepancy in line intensities is likely due to specific environmental effects.

It should be noted that the most intense bands for $Fe^{III}Cl_3$ and $Fe^{III}Br_3$ complexes with a maximum at about 438-491 nm in the experimental spectra (Fig. 3, compounds **1**-**4**) are the closest in position and intensity. An intense transition of the open form of the ligand is located in this range: the LUMO-HOMO type for TMI-NPS and a mixed transition with high oscillator strength LUMO – HOMO, LUMO-1 - HOMO for TMI-NSO with closely spaced LUMO and LUMO-1. It follows from the comparison that this high-intensity transition in the organic ligand also manifests itself in the complex.

For $Fe^{III}Br_3$ model complexes with a naphthalene-type ligand (Fig. S17), the positions of the bands change little, but their intensities change much more strongly when going to the corresponding $FeBr_3$ complexes with spiropyrans. This moment is especially pronounced for the band above 600 nm since these bands are not resolved. Energy and structural effects indicate the contribution of the zwitterionic configuration to the electronic structure of the ground state of spiropyrans. The same is true for excited states, which cause changes in intensities of optical transitions, which are very sensitive to configurational composition of state vectors.

The long-wavelength transition shifts to shorter wavelengths when going from TMI-NSO to TMI-NPS ligand as observed experimentally. These transitions are two-component. The energy gaps of beta LUMO - HOMO and alpha LUMO - HOMO are close, and corresponding transitions of different types simultaneously participate with approximately equal weights. The former of them is a ligand-metal transition and the latter is a metal-ligand one. These transitions

for naphthalene analogs of the TMI-NSO·$Fe^{III}Br_3$ and TMI-NPS·$Fe^{III}Br_3$ complexes contain presumably only the former ligand-metal component.

The calculated spectrum of the [($TMNOY^+$)($Fe^{III}Br_4^-$)] salt (Fig. S26, inset), which is the product of two electron oxidation and deprotonation reactions of TMI-NSO, is shown in Fig. S26. It is actually a superposition of the spectra of the $TMNOY^+$ cation and the $FeBr_4^-$ anion with slightly shifted peaks due to the transfer of an electron density of 0.18 e to the organic cation. All transitions of $Fe^{III}Br_4^-$ in the visible region are ligand-metal transitions involving half-filled d-orbitals of Fe^{III}. Only the transition with a maximum at 645 nm appears as a separate band, other transitions at 528, 454 and 416 nm overlap with more intense cation absorption peaks due to the HOMO-LUMO and HOMO-2-LUMO transitions (at 580 and 428 nm respectively for the isolated cation). In the $TMNOY^+$ cation, the C-C=N^+ fragment has a charge of +0.25 and only a fifth of it is located on the formally cationic nitrogen atom. 56% of LUMO is localized on the fragment N=C-C=N^+, and 53% of HOMO is localized on the naphthalene fragment

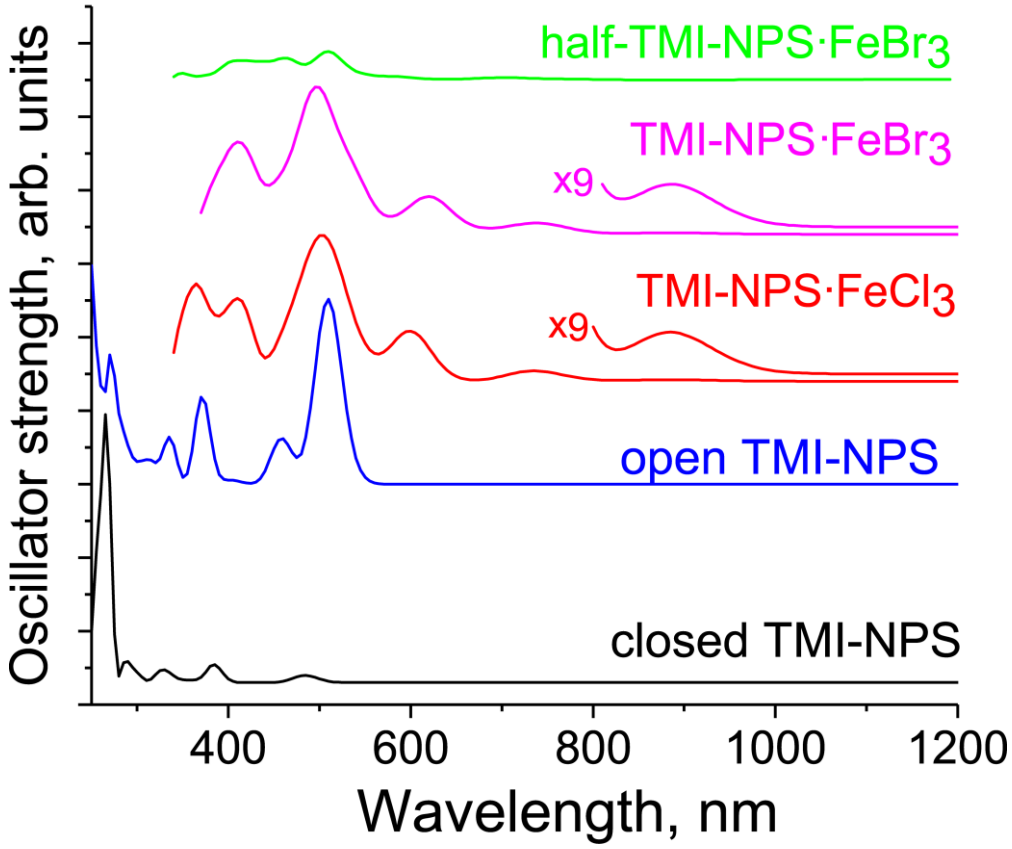

Fig. S24. Calculated spectra for TMI-NPS in the closed and open forms together with its coordination complexes in open form with $Fe^{III}Cl_3$ and $Fe^{III}Br_3$. Half-TMI-NPS ·$Fe^{III}Br_3$ indicates complex with the naphthalene analog of TMI-NPS (Fig. S17).

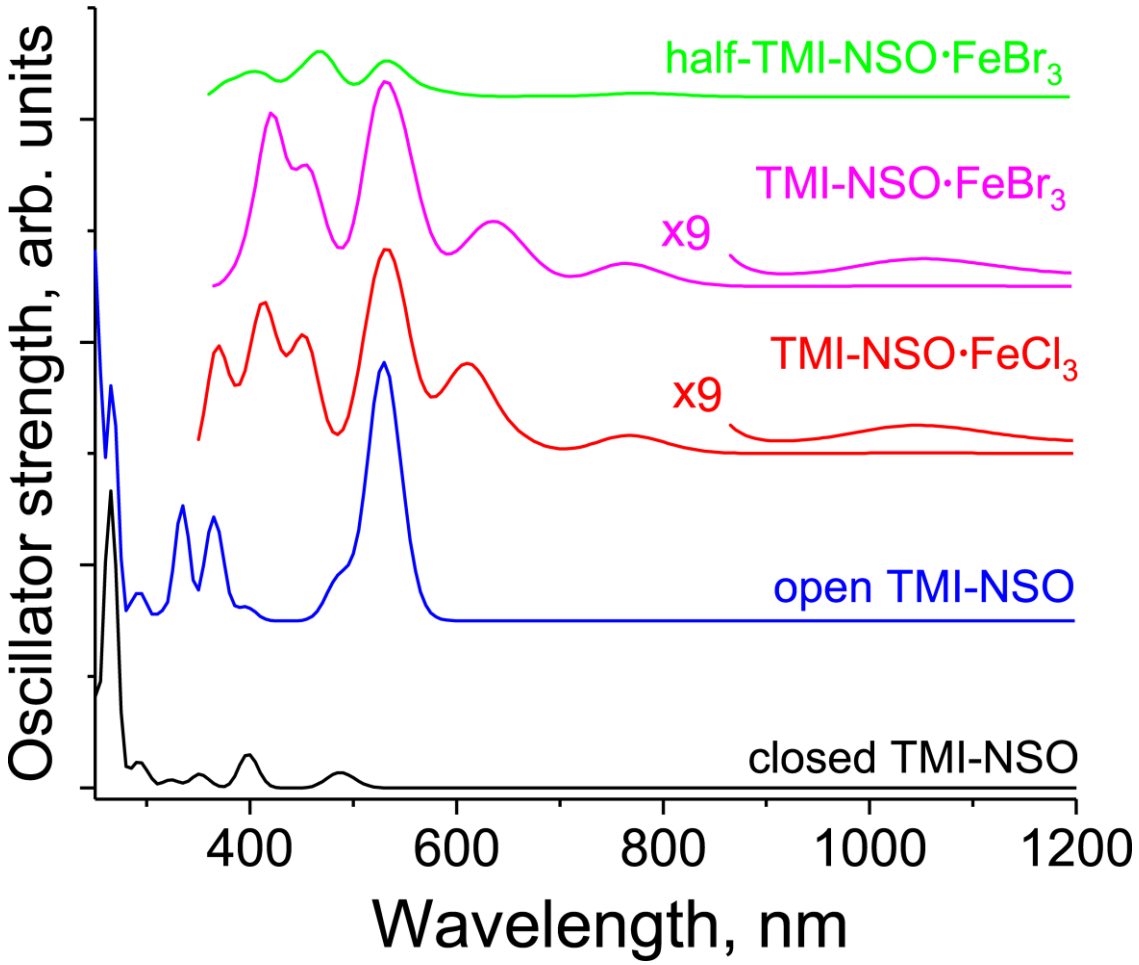

Fig. S25. Calculated spectra for TMI-NSO in closed and open forms together with its coordination complexes in the open form with $Fe^{III}Cl_3$ and $Fe^{III}Br_3$.

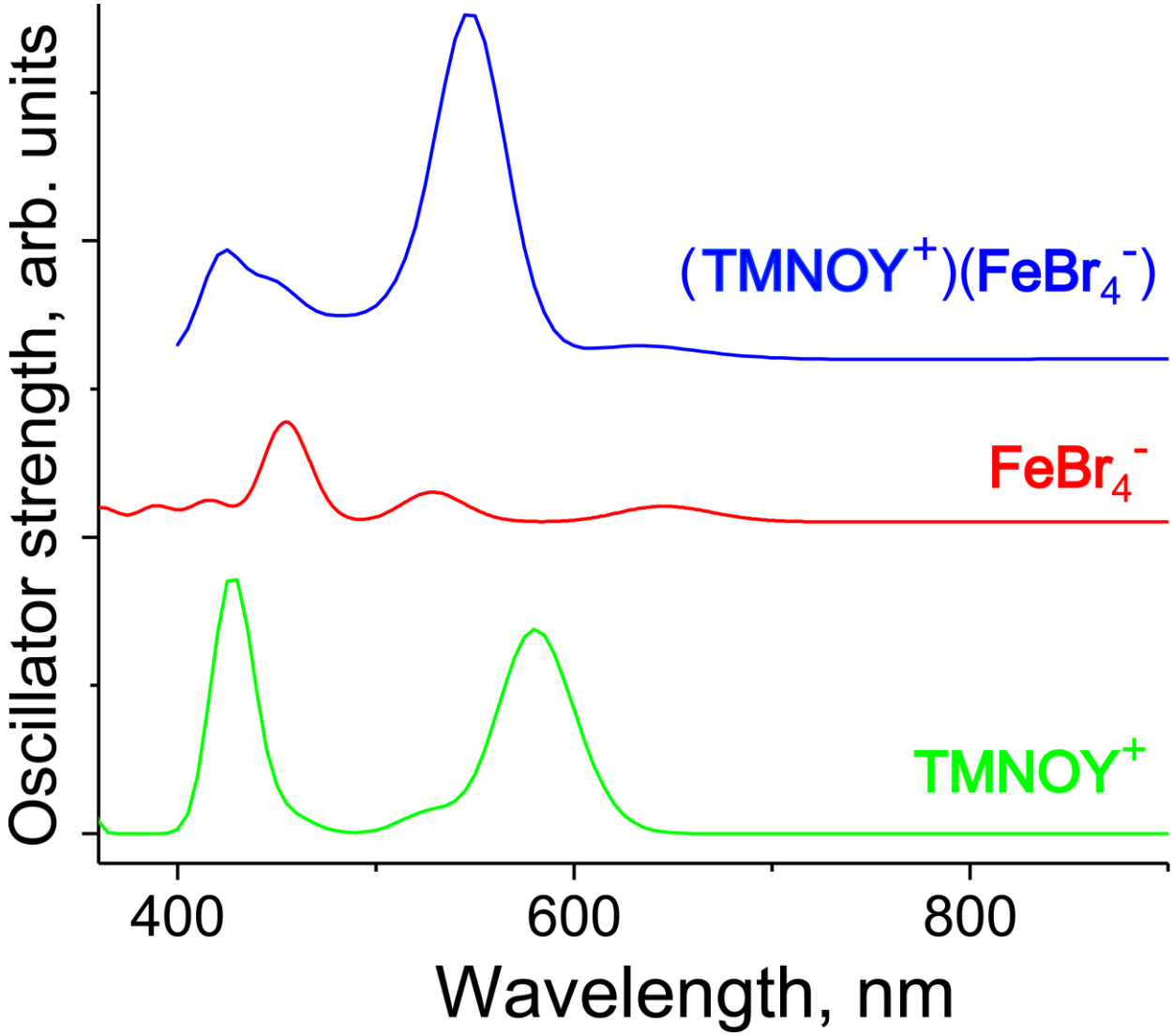

Fig. S26. Calculated spectra for oxidation product of TMI-NSO in form of $TMNOY^+$ cation, the $Fe^{III}Br_4^-$ anion and $(TMNOY^+)(Fe^{III}Br_4^-)$ salt. Inset shows molecular structure of the salt.

References

1 J. P. Perdew, K. Burke, M. Ernzerhof, *Phys. Rev. Lett.***1996**, *77*, 3865 – 3868.

2 W. J. Stevens, H. Basch, M. Krauss, *J. Chem. Phys*. **1984**, *81*, 6026 – 6033.

3 D. N. Laikov, *Chem. Phys. Lett.* **1997**, *281*, 151 – 156.

4 F. L. Hirshfeld, *Theor. Chim. Acta* **1977**, *44*, 129 – 138.

Cartesian coordinates of the optimized structures of the complexes

TMI-NPS·$FeBr_3$

6	0.88882854	1.24102944	0.17020941
6	2.28599810	0.59368524	0.21967488
6	3.17594258	1.81427706	0.40688902
6	4.55785320	1.92130608	0.52994988
1	5.19567428	1.03562440	0.49782643
6	5.12686383	3.19520457	0.69834647
1	6.20820759	3.29588696	0.79676819
6	4.31567380	4.33729795	0.74223854
1	4.77130814	5.31930345	0.87523797
6	2.92204520	4.24365563	0.61905166
1	2.30410864	5.14038080	0.65824373
6	2.37827034	2.96726308	0.45071923
7	1.02664791	2.59101744	0.30096425
6	-0.09125256	3.53183284	0.29703977
1	0.29601369	4.55396967	0.33702403
1	-0.74761494	3.36105625	1.16104744
1	-0.69095534	3.41436218	-0.61471218
6	2.43442981	-0.36109642	1.43134963
1	1.78290416	-1.23976635	1.33994171
1	2.18582888	0.15117025	2.37064363
1	3.47452032	-0.71131222	1.49744668
6	2.63610750	-0.11912980	-1.11142013
1	1.99126443	-0.98946861	-1.28938148
1	3.67874273	-0.46647610	-1.07842976
1	2.53019133	0.56381702	-1.96517727
6	-0.37784166	0.65624053	0.02584529
8	-3.17815583	0.52093268	-0.17854074
6	-3.09499635	-0.77032031	-0.29699662
6	-4.28507678	-1.55349804	-0.45430569
1	-5.23973162	-1.02711706	-0.46986882
6	-4.22532721	-2.91494675	-0.58168490
1	-5.14806210	-3.48820063	-0.70057578
6	-2.98307117	-3.62328097	-0.56441633
6	-2.96895852	-5.03295831	-0.69904912
1	-3.92211384	-5.55347653	-0.81496943
6	-1.77777305	-5.74177476	-0.68471266
1	-1.77500827	-6.82731989	-0.78887256
6	-0.56867588	-5.03686154	-0.53283496
1	0.37833206	-5.57926758	-0.51880657
6	-0.56152615	-3.65236091	-0.39921828
1	0.40707916	-3.16669293	-0.28449226
6	-1.75986510	-2.89383795	-0.40983927
6	-1.80308245	-1.43208526	-0.27228628
1	0.30377616	-1.33654410	-0.12205345
6	-0.59124257	-0.71738609	-0.12166683
1	-1.24707321	1.30958587	0.03152820
26	-4.67138212	1.78260650	-0.13853193
35	-5.81729227	1.56787912	-2.17875137
35	-3.71411093	3.93248227	0.11784294
35	-6.01642247	1.19331184	1.69576567

TMI-NSO·$FeBr_3$

6	0.52485397	0.03255764	1.37204946
6	1.90939441	-0.51384052	1.01885399
6	2.57112116	-0.54953968	2.38700532
6	3.84711878	-0.94806915	2.77447283
1	4.56735542	-1.31488538	2.04068804
6	4.19787665	-0.87069399	4.13288522
1	5.19401378	-1.17929506	4.45199654
6	3.28070678	-0.39944430	5.08302221
1	3.57013064	-0.34410400	6.13309951
6	1.99200154	0.00524709	4.70831432
1	1.29003600	0.37260305	5.45661690
6	1.66455991	-0.08273912	3.35264068
7	0.45079782	0.25084614	2.70979386
6	-0.72860191	0.77457409	3.39964266
1	-0.55139478	0.75764833	4.47880792
1	-1.61072477	0.16243614	3.17311706
1	-0.93621804	1.80559232	3.08320534
6	1.80944061	-1.93468244	0.40801777
1	1.26167068	-1.89736932	-0.54147749
1	1.28826157	-2.62413296	1.08665762
1	2.81999922	-2.32898740	0.22767765
6	2.65921050	0.44822210	0.06243997
1	2.12160237	0.52473207	-0.89044595
1	3.67294715	0.06493007	-0.12357372
1	2.74700934	1.45355646	0.49730358
6	-0.56529742	0.30105340	0.51709773
8	-3.10770039	1.03873712	-0.27116974
6	-2.73809022	0.73800887	-1.47562669
6	-3.64396626	0.87586605	-2.57684523
1	-4.64811647	1.24270656	-2.36047728
6	-3.26199899	0.56332547	-3.85621371
1	-3.97594563	0.68150483	-4.67517750
6	-1.94835532	0.08310279	-4.16048557
6	-1.57906559	-0.23199483	-5.49031815
1	-2.31684754	-0.10113441	-6.28488114
6	-0.30461438	-0.69871393	-5.78247206
1	-0.02746761	-0.93933640	-6.80962679
6	0.62864663	-0.85928750	-4.73934742
1	1.63217966	-1.22629114	-4.96232846
6	0.28594737	-0.55491353	-3.42534271
1	1.01256401	-0.68151977	-2.62441167
6	-1.00398733	-0.07792682	-3.10094316
6	-1.38288589	0.24886474	-1.72312094
7	-0.43550393	0.05921423	-0.78537520
1	-1.48601588	0.70017042	0.94911555
26	-4.77369398	1.64320432	0.56463513
35	-6.36723342	-0.03200426	0.16693716
35	-5.36039380	3.68325516	-0.43583166
35	-4.24532644	1.87894650	2.85939824

TMI-NPS·$FeCl_3$

6	0.88928345	1.23343584	0.17901801
6	2.29196900	0.59883575	0.21667438
6	3.17228565	1.82673747	0.40039866
6	4.55418082	1.94621967	0.51181022
1	5.19990691	1.06668649	0.47044028
6	5.11269398	3.22473039	0.68035035
1	6.19389528	3.33521302	0.76942602
6	4.29127688	4.35897001	0.73619041
1	4.73891962	5.34468151	0.86890144
6	2.89755142	4.25280347	0.62492367
1	2.27171661	5.14357831	0.67293558
6	2.36413841	2.97208896	0.45603358
7	1.01479199	2.58416970	0.31488176
6	-0.11221536	3.51492614	0.32779168
1	0.26754312	4.53994842	0.36189310
1	-0.75345915	3.33813187	1.20180727
1	-0.72503668	3.39246850	-0.57428983
6	2.45557789	-0.35646213	1.42623333
1	1.79978850	-1.23291326	1.34450463
1	2.22257014	0.15678862	2.36898941
1	3.49554239	-0.70965812	1.47681731
6	2.63769934	-0.10993142	-1.11747624
1	1.98891518	-0.97681393	-1.29788057
1	3.67908627	-0.46125088	-1.08713871
1	2.53309628	0.57692996	-1.96824270
6	-0.37332519	0.63995906	0.03759103
8	-3.15822176	0.52041014	-0.18466536
6	-3.08738844	-0.77075547	-0.30570402
6	-4.28327085	-1.54170611	-0.47650125
1	-5.23236717	-1.00582077	-0.50509850
6	-4.23346563	-2.90390887	-0.60140251
1	-5.15933371	-3.46986131	-0.73039153
6	-2.99720504	-3.62273122	-0.56976019
6	-2.99369489	-5.03284173	-0.70069091
1	-3.95004417	-5.54577837	-0.82390806
6	-1.80874545	-5.75155084	-0.67388316
1	-1.81441010	-6.83736367	-0.77513923
6	-0.59475520	-5.05672875	-0.51332670
1	0.34731872	-5.60734274	-0.48993326
6	-0.57694031	-3.67210516	-0.38258831
1	0.39434785	-3.19359717	-0.26052521
6	-1.76880971	-2.90386390	-0.40543811
6	-1.80088202	-1.44228877	-0.27068575
1	0.30776927	-1.35525098	-0.11235727
6	-0.58566338	-0.73337931	-0.11403919
1	-1.24479787	1.28982007	0.04609045
26	-4.63200506	1.80433482	-0.14845759
17	-5.69516754	1.60550309	-2.07215014
17	-3.63909359	3.77889657	0.09996279
17	-5.90156669	1.24763702	1.56800890

TMI-NSO·$FeCl_3$

6	0.48072536	0.06965663	1.38085641
6	1.89007796	-0.42634119	1.03694833
6	2.55225454	-0.42211180	2.40460992
6	3.84144950	-0.76233036	2.80443164
1	4.58246481	-1.10710847	2.08075907
6	4.17791831	-0.65301904	4.16475597
1	5.18428250	-0.91499932	4.49355414
6	3.23654440	-0.20986601	5.10528645
1	3.51872211	-0.13004569	6.15577554
6	1.93386183	0.13499390	4.71812746
1	1.20570619	0.48312747	5.45051554
6	1.62479508	0.01553033	3.36079369
7	0.39796203	0.29324695	2.71820293
6	-0.75941389	0.77626939	3.46984139
1	-0.92992188	0.11528511	4.33040457
1	-1.66230799	0.78586731	2.85287031
1	-0.56824948	1.79620913	3.83376724
6	1.84759457	-1.85719546	0.44281089
1	1.30331917	-1.85280119	-0.50922524
1	1.35084754	-2.55820909	1.12790705
1	2.87384343	-2.21345772	0.27214598
6	2.60418197	0.55408651	0.07201519
1	2.06950042	0.59651466	-0.88444081
1	3.63392837	0.21037572	-0.10318840
1	2.64834877	1.56757162	0.49443438
6	-0.60220116	0.28301354	0.50027633
8	-3.14785065	0.90321718	-0.32653617
6	-2.75294968	0.61321731	-1.52539425
6	-3.64879207	0.71720885	-2.63783997
1	-4.66761321	1.05021102	-2.43545768
6	-3.23835679	0.41146246	-3.91023937
1	-3.94363023	0.50195734	-4.74012352
6	-1.90541985	-0.02718302	-4.19275288
6	-1.50719041	-0.33740191	-5.51554371
1	-2.23755721	-0.23494831	-6.32106350
6	-0.21434294	-0.76388509	-5.78730339
1	0.08473252	-1.00103425	-6.80910104
6	0.70912712	-0.88831185	-4.73042440
1	1.72688863	-1.22414629	-4.93749871
6	0.33886750	-0.58750383	-3.42332268
1	1.05829636	-0.68601731	-2.61200294
6	-0.97039941	-0.15093416	-3.11934059
6	-1.37905834	0.17237464	-1.75036289
7	-0.43872044	0.02816346	-0.79496614
1	-1.54689199	0.65465847	0.90087161
26	-4.82462552	1.44880642	0.51862191
17	-6.28884591	-0.13940375	0.08669810
17	-5.38857976	3.38056950	-0.37810261
17	-4.25332217	1.58466022	2.66694886

Cartesian coordinates of the optimized structures and transition states of the TMI-NSO$^{\bullet-}$ radical cation transformation

Radical cation I

6	-0.14713723	0.94417982	0.01550159
6	-1.52524909	1.71944920	0.15920734
6	-1.34746306	2.35744140	1.53104450
6	-2.26205749	2.99697262	2.35323352
1	-3.31936818	3.04894944	2.08884228
6	-1.80664176	3.57386455	3.55589481
1	-2.51895171	4.06277344	4.22108000
6	-0.44574931	3.52069119	3.91694809
1	-0.12030154	3.97488870	4.85311616
6	0.49020227	2.88643767	3.10068191
1	1.53975581	2.83561116	3.38929210
6	0.02100974	2.31328542	1.90256165
7	0.75099512	1.66651569	0.92553646
6	2.16268291	1.33133914	1.03141177
1	2.71011360	2.18444068	1.45121651
1	2.56295661	1.12202294	0.03039737
1	2.32926103	0.45231579	1.67571133
6	-1.64415142	2.85441298	-0.89100938
1	-1.77588707	2.45040302	-1.90489500
1	-0.77318757	3.52553039	-0.88319670
1	-2.52835205	3.46246248	-0.65793564
6	-2.73577294	0.78077524	0.04426795
1	-2.75404016	0.28401111	-0.93714372
1	-3.66153448	1.36706864	0.12594621
1	-2.74457064	0.01556018	0.82869564
6	0.40277751	0.84945393	-1.39443173
8	-0.31243195	-0.38369780	0.60975390
6	0.13822538	-1.50064655	-0.01213740
6	0.09728471	-2.70804237	0.72000328
1	-0.28232196	-2.69846165	1.74176816
6	0.51746284	-3.87314150	0.10963005
1	0.47034294	-4.81586536	0.65788449
6	1.01033445	-3.88188182	-1.23098064
6	1.44413474	-5.07405880	-1.85509574
1	1.39629342	-6.01280452	-1.30017626
6	1.92778561	-5.05537195	-3.16196316
1	2.25802065	-5.98269233	-3.63143279
6	1.99060699	-3.84312147	-3.88202956
1	2.36823978	-3.84076535	-4.90503906
6	1.56954966	-2.65536150	-3.29998304
1	1.60384255	-1.71646955	-3.85187490
6	1.07289759	-2.64930073	-1.96710657
6	0.62641430	-1.45030966	-1.33380142
7	0.72940304	-0.23424586	-2.00594420
1	0.51457633	1.79538196	-1.93345017

Radical cation II

6	-0.62749329	1.20547840	-0.32482875
6	-1.64646071	2.31807160	-0.07409616

6	-1.11517733	2.91005204	1.21721031
6	-1.59357866	3.94253198	2.01871423
1	-2.50876042	4.47938579	1.76420196
6	-0.87168152	4.28307279	3.17439182
1	-1.23325328	5.08744392	3.81559731
6	0.30714633	3.60255270	3.52050315
1	0.84498471	3.88157363	4.42676652
6	0.80298742	2.56470598	2.72262703
1	1.71076516	2.03267847	3.00623622
6	0.06742168	2.24567318	1.57824131
7	0.34005630	1.24597231	0.60850081
6	1.55870976	0.44128827	0.63159000
1	2.34039774	1.00121395	1.15582082
1	1.89006123	0.24371840	-0.39356057
1	1.38533916	-0.51130612	1.15342691
6	-1.59962965	3.36162092	-1.22531875
1	-1.94197120	2.92160239	-2.17237006
1	-0.58916397	3.76835092	-1.36610683
1	-2.27418499	4.19354160	-0.98085956
6	-3.07743630	1.74505723	0.08288566
1	-3.11751178	0.97850153	0.86616522
1	-3.42508085	1.29870669	-0.85914829
1	-3.76709276	2.55918778	0.34482936
6	-0.72881162	0.33279655	-1.44201785
8	-1.45093429	-1.29867491	0.63173581
6	-0.71128498	-2.17815615	0.16519331
6	-0.61895395	-3.51884556	0.71304065
1	-1.28012835	-3.75050665	1.54798288
6	0.28653879	-4.41870483	0.23358884
1	0.35420477	-5.40850794	0.69172478
6	1.18380605	-4.12601524	-0.86383409
6	2.11650291	-5.08111612	-1.30785308
1	2.16445527	-6.05097977	-0.80934968
6	2.97083143	-4.79969106	-2.37812983
1	3.68817656	-5.55007838	-2.71211309
6	2.90102741	-3.55674078	-3.02670303
1	3.56114776	-3.34188162	-3.86762460
6	1.98308468	-2.59546670	-2.60157780
1	1.91643847	-1.63301725	-3.11124370
6	1.11802337	-2.86316392	-1.52072977
6	0.15211549	-1.87904510	-1.06001085
7	-0.08026017	-0.78310780	-1.73297653
1	-1.38537236	0.70022687	-2.24052204

Radical cation III

6	-1.13060693	0.88315794	-0.25471952
6	-1.17355774	1.35834830	1.18720990
6	-2.57732628	0.93540856	1.58671800
6	-3.27510534	1.05800945	2.78612474
1	-2.82180030	1.52164241	3.66363663
6	-4.59056700	0.56934755	2.84361164
1	-5.15305427	0.65687435	3.77366657

6	-5.19732060	-0.02861050	1.72768131
1	-6.22030593	-0.39768088	1.80216554
6	-4.50757426	-0.15948479	0.51495463
1	-4.97752902	-0.62703626	-0.35011696
6	-3.20330194	0.33199162	0.49091874
7	-2.27751683	0.33028162	-0.60008697
6	-2.63272683	-0.24867134	-1.90292009
1	-3.45240891	0.33539817	-2.34204316
1	-2.96589849	-1.28231335	-1.74406937
1	-1.76080796	-0.26216801	-2.55977255
6	-0.09192874	0.65805446	2.05472243
1	0.91572809	0.97294522	1.76013791
1	-0.16598357	-0.43536136	1.98973794
1	-0.24698283	0.95025721	3.10229785
6	-1.01702809	2.90665934	1.25338834
1	-0.01995044	3.21265003	0.91750635
1	-1.14910056	3.22209532	2.29730584
1	-1.77742455	3.41610548	0.64600707
6	0.02150820	0.94678738	-1.24407509
8	1.12818033	1.74103776	-0.70574549
6	2.21002735	0.90850064	-0.76637839
6	3.51831298	1.22195959	-0.41254217
1	3.79460427	2.21480179	-0.05991579
6	4.45916264	0.19683536	-0.53836603
1	5.49959494	0.39551663	-0.27618068
6	4.11553735	-1.11496882	-1.00264946
6	5.10059279	-2.12789803	-1.11798999
1	6.13242200	-1.89713071	-0.84666203
6	4.76318727	-3.39723608	-1.57217295
1	5.53226355	-4.16586157	-1.65673122
6	3.43196438	-3.69696828	-1.92770227
1	3.17872861	-4.69546886	-2.28593016
6	2.44087406	-2.72441549	-1.82739526
1	1.41052696	-2.94804824	-2.10604989
6	2.76301820	-1.43286137	-1.36622394
6	1.79367455	-0.37347240	-1.24170466
7	0.48584589	-0.39287244	-1.51999323
1	-0.30994703	1.46386257	-2.16965409

Radical cation IV

6	0.61686411	1.45626064	-0.34011121
6	-0.73495211	2.29321424	-0.37561838
6	-0.53158709	3.20112745	0.82253154
6	-1.24647284	4.32087419	1.22287771
1	-2.07560402	4.70185367	0.62495795
6	-0.89936291	4.95262452	2.43118184
1	-1.46461404	5.82297988	2.76568267
6	0.16336052	4.46932723	3.22566664
1	0.41080581	4.97937178	4.15694517
6	0.90552056	3.35963925	2.83699135
1	1.73384328	3.00458475	3.44871672
6	0.55401475	2.73492385	1.61772545

7	1.16785928	1.67597129	1.00676384
6	2.39323653	1.03332596	1.45768808
1	3.25391547	1.40416417	0.87552364
1	2.31003184	-0.05209206	1.33148159
1	2.55829974	1.25345451	2.51688547
6	-0.87562220	3.05524271	-1.70523333
1	-0.91850594	2.35266598	-2.55016566
1	-0.03614293	3.74566128	-1.86877250
1	-1.80716205	3.63767152	-1.71670906
6	-1.96981117	1.39354709	-0.13439655
1	-1.87206727	0.79559732	0.78133142
1	-2.12073884	0.71066799	-0.98321512
1	-2.86706494	2.02090223	-0.04307496
6	0.49966316	0.00960176	-0.69175542
8	0.62185104	-0.28962912	-2.03574048
6	0.46687795	-1.65867081	-2.08139825
6	0.47662356	-2.48445972	-3.21155752
1	0.62337407	-2.09476897	-4.21768984
6	0.28994145	-3.83876206	-2.96140972
1	0.29275603	-4.53852381	-3.79887983
6	0.09127935	-4.36333586	-1.64349905
6	-0.09973178	-5.75423642	-1.43355647
1	-0.08936128	-6.42578144	-2.29411932
6	-0.29828279	-6.26065460	-0.15392637
1	-0.44436661	-7.33183718	-0.01118109
6	-0.31345712	-5.39683141	0.96121028
1	-0.47270332	-5.80534391	1.95982580
6	-0.12795052	-4.02843108	0.79549208
1	-0.14019411	-3.35587146	1.65383070
6	0.07744080	-3.49255321	-0.49753656
6	0.27652878	-2.10840884	-0.76637759
7	0.30504318	-1.01438599	0.09165511
1	1.31662462	1.90932270	-1.06904078

Radical cation V

6	-1.10608545	0.54933290	-0.01880034
6	-2.01369717	1.06507512	1.11092458
6	-3.06706660	1.80713011	0.29997168
6	-4.18314117	2.52430267	0.71980223
1	-4.41931291	2.62830504	1.78022389
6	-5.00852388	3.12015854	-0.24837229
1	-5.88435712	3.68834097	0.06555106
6	-4.71606555	2.99618167	-1.61500426
1	-5.36484938	3.47033648	-2.35186496
6	-3.59922594	2.27436745	-2.05388349
1	-3.38107707	2.19746881	-3.11907057
6	-2.79321615	1.68732440	-1.07228459
7	-1.62925964	0.90818878	-1.24352354
6	-1.11899771	0.51541513	-2.54950931
1	-0.22947492	1.10227114	-2.83318112
1	-1.89179274	0.69597165	-3.30333778
1	-0.89569738	-0.56083682	-2.56507878

6	-2.65696243	-0.10152158	1.90696238
1	-1.89986183	-0.65946769	2.47235171
1	-3.18826994	-0.79525233	1.24133369
1	-3.38412566	0.30643079	2.62284063
6	-1.26538622	2.03158521	2.06314289
1	-0.48685392	1.50641374	2.63101135
1	-1.97836722	2.45709001	2.78291102
1	-0.80566403	2.86229169	1.51060734
6	0.07749839	-0.15163189	0.17627389
8	0.44236903	-0.54245831	1.43939150
6	1.66215244	-1.19477381	1.34714064
6	2.40170400	-1.74670253	2.39973078
1	2.05190912	-1.70630619	3.42977381
6	3.60308243	-2.34158206	2.04317019
1	4.22599213	-2.78944298	2.81860750
6	4.06597744	-2.39441204	0.69078016
6	5.30338262	-3.01073033	0.36447867
1	5.90122325	-3.44536184	1.16750193
6	5.74911354	-3.06336646	-0.94570073
1	6.70165639	-3.54050132	-1.17806047
6	4.97546157	-2.50356297	-1.98969252
1	5.33680006	-2.55473375	-3.01727653
6	3.76256049	-1.89259302	-1.71541686
1	3.17567162	-1.47130905	-2.53430381
6	3.28710758	-1.82373503	-0.38213409
6	2.06644472	-1.22186230	0.01739695
7	1.05834912	-0.58103274	-0.69709637
1	1.11887609	-0.30080529	-1.66828808

Transition state I-II

6	-0.46924542	1.06270380	-0.23861462
6	-1.69161740	1.96215658	0.11204434
6	-1.30406407	2.41443406	1.51382050
6	-2.02205854	3.10227130	2.48619121
1	-3.07169926	3.36149503	2.33806318
6	-1.36717088	3.45789184	3.67924895
1	-1.91775337	3.98865428	4.45635194
6	-0.01781272	3.13773415	3.88408726
1	0.46997250	3.42389814	4.81624397
6	0.71751549	2.44516104	2.91047715
1	1.76312776	2.18808188	3.08016906
6	0.04302767	2.09806045	1.73979427
7	0.54746144	1.40309838	0.60906467
6	1.92798218	0.94406025	0.51371863
1	2.59786218	1.74762293	0.84589535
1	2.16954863	0.69897007	-0.52657978
1	2.09593487	0.05957244	1.14851745
6	-1.66028770	3.20786144	-0.82394677
1	-1.96713810	2.94999461	-1.84777821
1	-0.67000945	3.68464971	-0.85043260
1	-2.37515993	3.94779703	-0.44139202
6	-3.05971018	1.27236474	0.00329354

1	-3.22253301	0.87455249	-1.00884331
1	-3.85063638	2.01104648	0.19453203
1	-3.16675691	0.45538732	0.72426542
6	-0.19429935	0.72132619	-1.66733575
8	-1.00025117	-0.57955958	0.35862989
6	-0.36952480	-1.61555929	-0.09177069
6	-0.34383291	-2.83214147	0.66028005
1	-0.90713140	-2.87337593	1.59224510
6	0.38586269	-3.90054610	0.20229251
1	0.40284708	-4.82867930	0.77759839
6	1.14660207	-3.84180523	-1.01682943
6	1.90628082	-4.93990213	-1.46070251
1	1.92326762	-5.85377205	-0.86406284
6	2.63230821	-4.86965116	-2.65550046
1	3.21518926	-5.73029991	-2.98545194
6	2.60247874	-3.70033464	-3.43736845
1	3.15907127	-3.65809811	-4.37394440
6	1.85428335	-2.60152518	-3.02606085
1	1.80008462	-1.70183773	-3.63940209
6	1.12428582	-2.64654383	-1.80841509
6	0.34518058	-1.53594779	-1.35506810
7	0.23793797	-0.41013204	-2.12132405
1	-0.41941988	1.49886483	-2.40600091

Transition state II-III

6	-0.67131594	1.13917296	-0.04400451
6	-1.72407422	2.19392798	0.27209683
6	-1.05751958	2.93233949	1.41682700
6	-1.48387715	4.01363921	2.18302858
1	-2.45408180	4.48211116	2.01031625
6	-0.63709690	4.49329517	3.19528698
1	-0.95666532	5.33701657	3.80758885
6	0.61346302	3.90112260	3.43608203
1	1.24982155	4.28850991	4.23192086
6	1.05800363	2.81542983	2.67299753
1	2.02532283	2.35710317	2.87662281
6	0.19940038	2.35860214	1.66879044
7	0.39644882	1.28554026	0.75995763
6	1.61521462	0.47797022	0.73974689
1	2.41082313	1.02093743	1.25818261
1	1.90607307	0.29475634	-0.30190210
1	1.44541118	-0.48745454	1.23823138
6	-1.95033864	3.13201032	-0.94578165
1	-2.39961850	2.58403691	-1.78610129
1	-1.01318909	3.59462546	-1.28317900
1	-2.64607672	3.93245819	-0.65916462
6	-3.06353291	1.53524023	0.70021351
1	-2.92775876	0.86646096	1.55934505
1	-3.49984644	0.95590895	-0.12440898
1	-3.77665673	2.32341532	0.97836572
6	-0.82589488	0.16322649	-1.09785091
8	-1.73081625	-1.29328407	-0.17823871

6	-0.92885111	-2.24070243	-0.50496804
6	-1.14637057	-3.62363811	-0.25658261
1	-2.05158478	-3.93291993	0.26414689
6	-0.17647969	-4.52999677	-0.63285196
1	-0.31738748	-5.58610082	-0.39249028
6	1.02586227	-4.15599240	-1.33055520
6	1.98348669	-5.12372201	-1.70393823
1	1.81059578	-6.17043074	-1.44705310
6	3.13357005	-4.75323081	-2.39986714
1	3.86408859	-5.51122224	-2.68425493
6	3.35110811	-3.40662375	-2.74273925
1	4.24748090	-3.12462022	-3.29615359
6	2.42190127	-2.43010313	-2.38354766
1	2.58203579	-1.38584420	-2.65606941
6	1.25758696	-2.78796535	-1.67637229
6	0.26166657	-1.82324247	-1.27734385
7	0.19106215	-0.56121634	-1.65133440
1	-1.61139390	0.44945303	-1.81299411

Transition state III-IV

6	-0.91336926	0.54826679	0.52963707
6	-0.97475338	1.83731120	1.38391687
6	-2.45487203	1.84197772	1.74506073
6	-3.21210273	2.77464556	2.44665996
1	-2.76984556	3.70123180	2.81655250
6	-4.57212481	2.50135030	2.67415754
1	-5.18130769	3.22358931	3.21804720
6	-5.15605411	1.31295753	2.21166741
1	-6.21292748	1.12193715	2.39929037
6	-4.40365173	0.36333758	1.50619579
1	-4.86177864	-0.55751093	1.14592460
6	-3.05751592	0.66184693	1.28823322
7	-2.09138793	-0.13486959	0.62280193
6	-2.41972829	-1.46203667	0.09949075
1	-2.83206138	-2.07437647	0.91323817
1	-1.51984133	-1.92865484	-0.30827924
1	-3.17495258	-1.37136270	-0.69576524
6	-0.11475719	1.65082006	2.66511081
1	0.95449471	1.60475432	2.42253710
1	-0.39997690	0.74195454	3.21271883
1	-0.28079039	2.50943789	3.32950862
6	-0.55717761	3.10947135	0.61627478
1	0.50347581	3.07949992	0.33621813
1	-0.70681811	3.98671049	1.26011361
1	-1.16715441	3.25077918	-0.28755374
6	0.26769533	0.08106909	-0.18421498
8	1.46513522	0.77987724	0.04696432
6	2.40792178	0.04963549	-0.64083525
6	3.76444811	0.33202082	-0.76540305
1	4.22106286	1.20962854	-0.31051053
6	4.50517276	-0.58804083	-1.50871959
1	5.57615325	-0.42362133	-1.63832692

6	3.92040555	-1.74646653	-2.11616152
6	4.71375283	-2.65152325	-2.86527208
1	5.78230144	-2.45689694	-2.97320480
6	4.14304148	-3.77287098	-3.45748396
1	4.76616047	-4.46005868	-4.03075712
6	2.76299827	-4.02672574	-3.32257581
1	2.32633623	-4.90854105	-3.79268130
6	1.95419880	-3.15905163	-2.59328869
1	0.88618830	-3.35153396	-2.48686907
6	2.51436551	-2.01733564	-1.98430121
6	1.75987360	-1.07319668	-1.21599821
7	0.43484615	-1.04994306	-0.91659027
1	-0.59507898	0.94050667	-0.79552772

Transition state III-V

6	-0.57934232	0.29960628	1.03185010
6	-0.25536857	1.28609219	2.16227702
6	-1.46750707	1.08820429	3.05924927
6	-1.81700207	1.68833733	4.26556793
1	-1.18843096	2.45616825	4.71972864
6	-3.00722582	1.28637637	4.89500964
1	-3.29905377	1.75024424	5.83756005
6	-3.82609300	0.29675928	4.32988377
1	-4.74415875	0.00071863	4.83793957
6	-3.48411242	-0.32022015	3.11925103
1	-4.12230038	-1.08925572	2.68452829
6	-2.30007829	0.10347136	2.51118753
7	-1.73122483	-0.36298899	1.29885505
6	-2.36383283	-1.44600751	0.54178192
1	-2.44548356	-2.33282492	1.18554756
1	-1.76885021	-1.68039234	-0.34324718
1	-3.37328382	-1.13609898	0.23531259
6	1.04385623	0.87370730	2.91011383
1	1.92469687	0.98413137	2.26625950
1	0.98818262	-0.16313685	3.26832130
1	1.17283351	1.52763910	3.78355428
6	-0.15351923	2.74371953	1.64804326
1	0.70600640	2.86805659	0.97642026
1	-0.01267810	3.41953208	2.50261078
1	-1.06881934	3.04878320	1.12258523
6	0.15726764	0.22529429	-0.18835306
8	1.47443722	0.70053635	-0.19716625
6	2.04422866	0.20273469	-1.35318915
6	3.34316464	0.44548985	-1.80557572
1	4.04982775	1.04693422	-1.23638105
6	3.67496595	-0.13493316	-3.02540579
1	4.67986503	0.01114131	-3.42509816
6	2.75201986	-0.91589684	-3.78992677
6	3.12992056	-1.48252416	-5.03547903
1	4.14508930	-1.32284605	-5.40306059
6	2.22535859	-2.22739529	-5.77646626
1	2.52820070	-2.65599506	-6.73236752

6	0.91012727	-2.43684130	-5.30202124
1	0.20955696	-3.02407090	-5.89684633
6	0.50455603	-1.90395797	-4.08639789
1	-0.50893246	-2.06808231	-3.71889606
6	1.41038803	-1.14012158	-3.31546739
6	1.09293752	-0.55650604	-2.05295985
7	-0.09802001	-0.60244547	-1.35028612
1	-0.55216950	0.64886352	-1.15884699

Cartesian coordinates of the optimized structures and transition states of the charge transfer (TMI-NSO$^{\bullet+}$)($Fe_2Br_6^-$) adduct transformation

Charge transfer adduct Ic

26	2.38739327	2.56898326	-5.40629584
35	0.78123110	2.81008969	-7.06653886
35	4.53348771	1.90512272	-5.99932224
26	1.70438768	3.08176612	-2.53116356
35	1.52829260	0.94671531	-3.75747999
35	-0.44527658	3.71414057	-1.80180343
35	2.54519610	4.70069410	-4.15672997
35	3.31165655	2.82582689	-0.81429906
6	-0.70690937	0.11153662	1.14199508
6	-1.98173915	0.91566973	1.64050408
6	-1.38193036	2.28157086	1.91580537
6	-1.99056846	3.50478176	2.15652436
1	-3.07499672	3.61276135	2.10274017
6	-1.18417388	4.61579182	2.46506893
1	-1.65065789	5.58472173	2.64608411
6	0.21784542	4.50053129	2.52745060
1	0.82021767	5.38224585	2.74781257
6	0.85243718	3.28364457	2.28543965
1	1.93851790	3.20213277	2.29273779
6	0.03313338	2.17723164	1.98333964
7	0.42589369	0.89205882	1.70617253
6	1.80867442	0.45769962	1.62241968
1	2.33404562	0.96964202	0.79216978
1	1.84412777	-0.62631097	1.47039521
1	2.32676228	0.69800880	2.56183875
6	-3.12108754	0.91944007	0.60815015
1	-3.42318606	-0.10963427	0.36308134
1	-2.84763224	1.43709328	-0.32014518
1	-4.00181041	1.42588162	1.02825449
6	-2.49289459	0.32024111	2.97744482
1	-2.90169484	-0.68696612	2.82358908
1	-3.29131610	0.96563570	3.36921836
1	-1.69731148	0.26060575	3.73220882
6	-0.52721330	0.12654432	-0.38062840
8	-0.71150557	-1.20823782	1.66963181
6	-0.28289412	-2.27168965	0.90151567
6	-0.17571532	-3.51709902	1.55462988
1	-0.40869118	-3.58141784	2.61796675

6	0.22280175	-4.62535469	0.82828733
1	0.31511042	-5.59210408	1.32730731
6	0.51659207	-4.53831820	-0.56161930
6	0.92949562	-5.67314424	-1.31211002
1	1.02597069	-6.63445773	-0.80295742
6	1.20368300	-5.56189822	-2.66357838
1	1.52059454	-6.43749862	-3.23191250
6	1.07460127	-4.31050633	-3.31408142
1	1.29278948	-4.23182672	-4.38030388
6	0.67730607	-3.18331184	-2.61306000
1	0.58214590	-2.21825795	-3.11062502
6	0.39013506	-3.27085712	-1.22669641
6	-0.02235012	-2.13107129	-0.46009757
7	-0.19634207	-0.89397065	-1.08151031
1	-0.62662884	1.10512360	-0.86682537

Transition state Ic-IIc

26	2.43702768	2.91375788	-5.62158246
35	0.99164101	3.91976055	-7.13919412
35	4.35289785	1.84871079	-6.40245768
26	2.00324069	2.79938065	-2.66057914
35	1.10957260	1.24229062	-4.36173028
35	0.16610618	3.64032255	-1.41974529
35	3.07844738	4.60343968	-3.93422832
35	3.60595815	1.69259159	-1.33746710
6	-1.25467792	0.30037724	0.47379429
6	-2.75417524	0.60437583	0.76003440
6	-2.67125670	1.03799062	2.21671080
6	-3.66299795	1.28972146	3.15874997
1	-4.71660974	1.12482100	2.92547887
6	-3.28435509	1.76455075	4.42761200
1	-4.04936455	1.96112104	5.17961441
6	-1.93652337	1.98980791	4.73476638
1	-1.66169716	2.36108053	5.72284945
6	-0.92641288	1.73976952	3.79201361
1	0.12213096	1.90834229	4.03723082
6	-1.32670577	1.26052775	2.54516739
7	-0.51584256	0.93077763	1.43082701
6	0.93527671	1.07949363	1.44097483
1	1.19128393	2.05945626	1.86348373
1	1.33118424	1.04590413	0.42013886
1	1.40374238	0.28984231	2.04981656
6	-3.17188509	1.83982761	-0.09184588
1	-3.27122950	1.57605986	-1.15457654
1	-2.45823686	2.66962203	-0.00058167
1	-4.15163451	2.18919135	0.26048870
6	-3.72139607	-0.55632213	0.48342638
1	-3.53232996	-1.41364355	1.13737895
1	-3.64521036	-0.88890713	-0.56185816
1	-4.75272528	-0.21029945	0.64383078
6	-0.77228093	0.20463116	-0.93292803
8	-1.13886508	-1.49523256	0.93473192

6	-0.09984662	-2.13622354	0.49867309
6	0.34083047	-3.32792315	1.15800361
1	-0.24610397	-3.69270868	2.00099695
6	1.48696437	-3.96047674	0.74246791
1	1.82388511	-4.86256103	1.25852996
6	2.27736613	-3.46643918	-0.34886773
6	3.46505495	-4.11276870	-0.74905616
1	3.79088527	-5.00528091	-0.21078614
6	4.21776426	-3.62230539	-1.81782471
1	5.13678595	-4.13034907	-2.11320144
6	3.79262523	-2.47669974	-2.51526485
1	4.38194737	-2.09207392	-3.34834867
6	2.62178642	-1.82069958	-2.14586655
1	2.28888790	-0.93665590	-2.68911026
6	1.84770902	-2.29731083	-1.05741086
6	0.63656473	-1.64619555	-0.64834278
7	0.13104471	-0.60817471	-1.37475483
1	-1.24624846	0.87170525	-1.66018197

Transition state IIc-IIIc

26	0.39843898	3.86156322	-4.57888780
35	-1.66693999	4.88371032	-4.93886265
35	1.59106851	3.18129305	-6.46250791
26	1.41131830	3.38969287	-1.69858280
35	0.04323150	1.86982334	-3.11082825
35	0.12017536	4.08323511	0.17305752
35	1.83354690	5.31453312	-3.16726998
35	3.42031866	2.30414197	-1.10018377
6	-1.09132496	0.20951281	0.76051228
6	-2.54435976	0.58257119	1.01348966
6	-2.42096865	1.37583268	2.29794119
6	-3.37430468	1.99933255	3.09860938
1	-4.43704696	1.95074549	2.85587325
6	-2.93649628	2.70782112	4.22895452
1	-3.66840004	3.20563695	4.86615143
6	-1.57171164	2.79835867	4.54770645
1	-1.25881312	3.36724256	5.42358281
6	-0.60206062	2.17901698	3.75092682
1	0.45845713	2.26609502	3.98368332
6	-1.06591230	1.47076391	2.64129434
7	-0.30022984	0.75076360	1.68555609
6	1.16525018	0.76798814	1.73770122
1	1.49363940	1.80971373	1.60623552
1	1.56501998	0.16780303	0.91734261
1	1.49157152	0.38569128	2.71431086
6	-3.02791852	1.49734288	-0.15448491
1	-3.05977515	0.93958198	-1.10069065
1	-2.37472193	2.37111868	-0.28045824
1	-4.04600564	1.84406128	0.07130018
6	-3.47179756	-0.64824972	1.15569741
1	-3.13811949	-1.31607708	1.96002009
1	-3.51094870	-1.22454804	0.22241053

1	-4.48885785	-0.30091156	1.38506554
6	-0.68835278	-0.67564407	-0.33969233
8	-1.07015580	-2.38597302	0.16201532
6	0.00681476	-2.97288096	-0.28552270
6	0.30737411	-4.35071752	-0.16921905
1	-0.40280559	-5.02034979	0.31465891
6	1.48846120	-4.81860898	-0.72081474
1	1.71021175	-5.88700963	-0.67299972
6	2.44450910	-3.96193904	-1.36635336
6	3.63856759	-4.47672445	-1.92285717
1	3.83270807	-5.54968103	-1.86402901
6	4.55613974	-3.62928169	-2.53756686
1	5.47255080	-4.03973803	-2.96406669
6	4.30792031	-2.24425986	-2.61344601
1	5.03100942	-1.58574307	-3.09617511
6	3.13932342	-1.70699921	-2.07864221
1	2.94060262	-0.63470748	-2.13583770
6	2.20106642	-2.55367302	-1.45292792
6	0.97088027	-2.06149308	-0.89201333
7	0.61644287	-0.79398598	-0.72306704
1	-1.43859104	-0.69579123	-1.14610930

Charge transfer adduct IIc

26	1.27187505	2.86438151	-4.49070399
35	-0.35759859	3.52890157	-6.01914531
35	3.10800495	1.66382975	-5.30162747
26	1.32573609	3.25893293	-1.50230878
35	0.16647186	1.45121754	-2.75400063
35	-0.26977313	4.20507566	-0.03866664
35	2.05849451	4.84541161	-3.22297955
35	3.22756335	2.37713443	-0.39352577
6	-1.15797063	0.12483580	1.09578980
6	-2.59735290	0.59626497	1.28208629
6	-2.42849198	1.62109650	2.38464642
6	-3.34962525	2.44136395	3.02874605
1	-4.40918147	2.41290334	2.76958840
6	-2.88488668	3.32370227	4.01733338
1	-3.59160131	3.97923997	4.52748828
6	-1.52168295	3.38784622	4.34902704
1	-1.18343530	4.09549216	5.10636216
6	-0.58381465	2.56912128	3.71089559
1	0.47656490	2.64256877	3.94847009
6	-1.07230374	1.69083531	2.74010205
7	-0.34490995	0.76073122	1.95995732
6	1.10212585	0.60587888	2.09147412
1	1.61879548	1.36015339	1.47156882
1	1.39545493	-0.38639169	1.74002023
1	1.37649286	0.74056471	3.14445319
6	-3.13396739	1.24311713	-0.02323983
1	-3.19648451	0.49916715	-0.82952475
1	-2.49090265	2.06969844	-0.35324446
1	-4.14502788	1.63403061	0.15879909

6	-3.50712327	-0.58090686	1.72445273
1	-3.14544816	-1.04296646	2.65301403
1	-3.55382028	-1.35579701	0.94737550
1	-4.52539872	-0.20530817	1.89724693
6	-0.81109408	-0.87397927	0.14591009
8	-1.19846371	-3.50576758	0.05790599
6	-0.10502440	-3.60080947	-0.52879121
6	0.40819464	-4.86052756	-1.03901907
1	-0.20536326	-5.74405803	-0.86230348
6	1.58502265	-4.91945464	-1.72610864
1	1.93492817	-5.87896166	-2.11610134
6	2.39895263	-3.75460845	-1.98733731
6	3.57498515	-3.84801015	-2.75344981
1	3.87922785	-4.82131208	-3.14390372
6	4.33985662	-2.70987086	-3.02664400
1	5.24221540	-2.79489750	-3.63362096
6	3.94303629	-1.45706168	-2.53159188
1	4.52591735	-0.56358040	-2.75733203
6	2.78563265	-1.34182158	-1.76273993
1	2.47838463	-0.36552521	-1.38527129
6	1.99992342	-2.48147030	-1.47892713
6	0.77102134	-2.37889225	-0.72185748
7	0.42559085	-1.23975750	-0.14217600
1	-1.64972262	-1.28176072	-0.42657117

Charge transfer adduct IIIc

26	1.43023349	1.30773123	-5.00698058
35	-0.84466256	0.73103032	-4.67594394
35	2.18962254	1.11550827	-7.19335492
26	3.46502914	2.29240351	-2.97696134
35	2.88048354	-0.05900501	-3.50743811
35	3.11910931	2.63298215	-0.61719408
35	1.77070467	3.62531628	-4.18390309
35	5.61005154	2.78875059	-3.70957024
6	0.17589560	0.94321676	0.68933326
6	-1.04452264	1.77711621	0.34476828
6	-1.05777900	2.75252271	1.50767080
6	-1.91242150	3.80711582	1.82058723
1	-2.76444034	4.05199172	1.18449185
6	-1.64662183	4.56230015	2.97389522
1	-2.30280494	5.39429917	3.23217378
6	-0.54624339	4.27340723	3.79575080
1	-0.35663341	4.88308229	4.67949245
6	0.32093020	3.21472805	3.49402782
1	1.18361355	2.99892356	4.12369716
6	0.02635836	2.47900425	2.34777372
7	0.73290174	1.36036964	1.80778801
6	1.96172448	0.84439859	2.42489959
1	2.79377138	1.50715553	2.14878476
1	2.13987816	-0.17519804	2.07329430
1	1.82725009	0.83550060	3.51299932
6	-0.84744342	2.52161768	-1.01005487

1	-0.82793154	1.81550678	-1.84929126
1	0.08207549	3.10519283	-1.01370673
1	-1.69676771	3.20547333	-1.14766102
6	-2.33133052	0.90665518	0.30747851
1	-2.47310856	0.34594652	1.24148671
1	-2.30366066	0.21075823	-0.53837396
1	-3.19384044	1.57342168	0.17109858
6	0.76431659	-0.22816972	-0.07565376
8	0.01350446	-0.45297228	-1.30672718
6	-0.29721370	-1.77370623	-1.28980042
6	-0.94557208	-2.48519274	-2.29838454
1	-1.23045323	-1.99961072	-3.23194559
6	-1.18181571	-3.83636037	-2.04913074
1	-1.67931381	-4.43937543	-2.81071109
6	-0.78938225	-4.47856980	-0.82695892
6	-1.04752677	-5.85556098	-0.60825467
1	-1.55521597	-6.42732608	-1.38778065
6	-0.66149447	-6.47400047	0.57419473
1	-0.86719273	-7.53481655	0.72463781
6	-0.00104570	-5.73856626	1.58111340
1	0.30130361	-6.23365681	2.50501503
6	0.26985799	-4.38662511	1.39750049
1	0.78503382	-3.81025820	2.16697494
6	-0.11697289	-3.74092940	0.20562953
6	0.13505499	-2.34523745	-0.05419782
7	0.74771918	-1.44144112	0.71629307
1	1.79698783	0.05315192	-0.38287162

Transition state IIIc-IVc

26	0.93650896	0.82535622	-5.12715651
35	-1.36626282	0.75691654	-4.64630585
35	1.56301611	0.86700036	-7.35907737
26	3.14297615	0.86094934	-3.12000142
35	2.01888254	-1.12167756	-3.99546670
35	2.83244611	0.77655680	-0.61193816
35	1.90433389	2.80205333	-3.94384193
35	5.42205795	0.95589133	-3.50802673
6	-0.33867002	1.00775530	1.01490646
6	-1.16866644	2.16908796	0.44796780
6	-0.99747502	3.20399190	1.54985883
6	-1.48242893	4.50314718	1.66598949
1	-2.09547248	4.94709085	0.87945219
6	-1.16567568	5.24228803	2.81920523
1	-1.53736369	6.26215907	2.92387963
6	-0.37577055	4.68540426	3.83442957
1	-0.13831431	5.27591380	4.72014485
6	0.12092367	3.37749446	3.73007172
1	0.73925079	2.94895687	4.51875414
6	-0.20870264	2.66642030	2.57461018
7	0.15861443	1.34270838	2.23290064
6	0.98863721	0.53308140	3.12462055
1	1.96965539	1.01513643	3.24949944

1	1.10908620	-0.46569181	2.69579222
1	0.50103898	0.46030226	4.10757283
6	-0.63779543	2.69891492	-0.90691133
1	-0.73772927	1.94801903	-1.70030057
1	0.41388976	3.00463504	-0.83371385
1	-1.22868701	3.57827703	-1.19975627
6	-2.65808620	1.74594409	0.31714364
1	-3.05362968	1.36601809	1.26962120
1	-2.77720863	0.97795824	-0.45666525
1	-3.25286381	2.62279768	0.02505044
6	-0.05693559	-0.22084703	0.33841735
8	-0.73838233	-0.42326402	-0.89490692
6	-0.64037792	-1.76747921	-1.11691679
6	-1.11989347	-2.47554129	-2.22347850
1	-1.61041720	-1.96843154	-3.05384622
6	-0.90992651	-3.84908363	-2.20281996
1	-1.26055356	-4.45406727	-3.04076981
6	-0.23268226	-4.51293563	-1.12711047
6	-0.03012576	-5.91789465	-1.14523472
1	-0.40382770	-6.49273422	-1.99513279
6	0.63359394	-6.55540873	-0.10721951
1	0.78232825	-7.63581404	-0.13927128
6	1.12250676	-5.81313229	0.99117304
1	1.64656239	-6.32417313	1.80020780
6	0.94199667	-4.43718631	1.04297286
1	1.31927385	-3.85537166	1.88486192
6	0.26794530	-3.76896783	-0.00268390
6	0.03780279	-2.35365875	-0.02396038
7	0.36818836	-1.40366500	0.88707651
1	1.28240848	0.38879909	-0.16366735

Ion pair IVc

26	1.69652974	0.80573522	-4.70038420
35	-0.65697745	0.63821162	-4.65911559
35	2.83799358	0.52562120	-6.69905045
26	3.61053271	1.34829424	-2.66784394
35	2.57447865	-0.83826386	-3.00796139
35	3.02460565	1.64147486	-0.03637786
35	2.26680798	3.06141675	-3.72963956
35	5.92286900	1.50872830	-2.59740735
6	-0.78260025	0.87982218	0.98317407
6	-1.66275858	1.96454348	0.34094415
6	-1.63622996	3.03060294	1.42649887
6	-2.22156399	4.29169184	1.47849957
1	-2.81634200	4.66950295	0.64472554
6	-2.03243900	5.08016877	2.62732310
1	-2.48442113	6.07113477	2.68127986
6	-1.26751172	4.60752911	3.70332542
1	-1.13045202	5.23438600	4.58536295
6	-0.67001446	3.33968644	3.66544446
1	-0.07291300	2.97746938	4.50235686
6	-0.87345183	2.57520394	2.51224930

7	-0.38609927	1.28444921	2.23210784
6	0.43018716	0.55346786	3.19689568
1	1.36382731	1.10488946	3.38755115
1	0.65871467	-0.43827851	2.79678654
1	-0.12072129	0.45853349	4.14440133
6	-1.07577551	2.50498704	-0.98756226
1	-1.03663899	1.72569955	-1.75935174
1	-0.06653596	2.91434310	-0.84406263
1	-1.71532190	3.31790236	-1.36032105
6	-3.11159453	1.45059989	0.11854942
1	-3.54087142	1.04984485	1.04739991
1	-3.13418800	0.67150799	-0.65307673
1	-3.74214971	2.28599543	-0.21747009
6	-0.48343323	-0.37945691	0.41314702
8	-1.01519036	-0.63912543	-0.85389450
6	-0.59101884	-1.90603270	-1.14797547
6	-0.85111966	-2.64156463	-2.31180990
1	-1.41443201	-2.21973096	-3.14279691
6	-0.30956256	-3.91768643	-2.34857535
1	-0.46562507	-4.53691002	-3.23366306
6	0.47116799	-4.46072518	-1.27483756
6	1.01211954	-5.77114595	-1.35361230
1	0.82410673	-6.36516582	-2.25036487
6	1.77055404	-6.29181667	-0.31610803
1	2.18050662	-7.29983510	-0.39461199
6	2.01939047	-5.52264491	0.84345314
1	2.61932935	-5.94205685	1.65252985
6	1.50817899	-4.23719355	0.95577408
1	1.69846195	-3.63592659	1.84567612
6	0.73283678	-3.68722314	-0.09000222
6	0.16634715	-2.37427734	-0.05913311
7	0.22300068	-1.40447428	0.90674124
1	1.75540697	0.93609061	0.00481261

Ion pair IVci

26	1.60918472	-3.33894447	3.54066067
35	0.38355914	-2.92931196	1.30717646
35	3.91210918	-3.35868724	3.18308209
26	-0.75466850	-3.19707075	5.08500715
35	0.42223958	-5.28076961	4.39976682
35	-2.42845248	-2.79670923	3.31745443
35	0.89823447	-1.34924454	4.85375199
35	-1.49683337	-3.34180232	7.28702216
6	-0.87921314	0.83573477	0.00662292
6	-2.40893933	0.86958227	-0.11420123
6	-2.79997544	1.17910559	1.32221263
6	-4.04847363	1.33153573	1.91668805
1	-4.96677669	1.23774886	1.33393407
6	-4.10973155	1.60061154	3.29488780
1	-5.08063457	1.71539021	3.77806540
6	-2.93933663	1.71083512	4.06002243

1	-3.00993115	1.90342251	5.13100655
6	-1.67517490	1.56263375	3.47487151
1	-0.76810359	1.63000052	4.07433423
6	-1.64157603	1.29990920	2.10259373
7	-0.50804495	1.10135400	1.28679416
6	0.83967233	1.14039203	1.84934151
1	1.00281577	2.11808253	2.32539820
1	1.57006122	0.97714300	1.05404290
1	0.93186980	0.35302666	2.61493302
6	-2.87718848	2.00132914	-1.06742494
1	-2.57097682	1.79684302	-2.10093651
1	-2.46851738	2.97402877	-0.76086219
1	-3.97412348	2.06795552	-1.03803275
6	-2.99033022	-0.49682070	-0.56196592
1	-2.67405941	-1.30327532	0.11260824
1	-2.67632000	-0.74285950	-1.58369561
1	-4.08838867	-0.44645047	-0.53843451
6	0.02310102	0.59044773	-1.05871147
8	-0.54243051	0.33171548	-2.31476181
6	0.53603528	0.13605005	-3.13521720
6	0.52472775	-0.15675178	-4.50607694
1	-0.40305663	-0.26190285	-5.06693993
6	1.76921164	-0.30599016	-5.10163914
1	1.82689216	-0.53548152	-6.16718885
6	2.99662827	-0.17532378	-4.37275902
6	4.25188373	-0.34078575	-5.01670477
1	4.27074388	-0.56820012	-6.08462839
6	5.43575671	-0.22045324	-4.30602461
1	6.39167638	-0.35301770	-4.81490322
6	5.41364665	0.06883884	-2.92203042
1	6.35204233	0.15445457	-2.37226091
6	4.20692831	0.23917421	-2.25868499
1	4.18132279	0.45582219	-1.19021358
6	2.98782613	0.12351370	-2.96477025
6	1.70034845	0.28088809	-2.36367026
7	1.35282907	0.56834628	-1.06853011
1	-1.01008922	-2.85606285	2.13899045

Cartesian coordinates of ion pair $[(C_{22}H_{19}N_2O^+)(FeBr_4^-)]$

6	-0.94277304	0.88369340	0.09860693
6	-1.28177664	2.03650982	1.04034493
6	-2.79405423	2.04947184	0.92941513
6	-3.74456116	2.87162312	1.52773590
1	-3.44887647	3.67829304	2.20067293
6	-5.10122939	2.63659039	1.25497288
1	-5.86048811	3.26870807	1.71687827
6	-5.49526835	1.59351205	0.40290891
1	-6.55510031	1.42232005	0.21246071
6	-4.54978100	0.75661397	-0.20146272
1	-4.86659638	-0.05916263	-0.84942194
6	-3.20701786	1.01334460	0.08138742
7	-2.05676103	0.32872531	-0.39442970

6	-2.12977230	-0.84753145	-1.26653594
1	-3.17680732	-1.14677916	-1.35583228
1	-1.55068619	-1.67367214	-0.82729059
1	-1.71005776	-0.60721175	-2.25162259
6	-0.84254505	1.70603047	2.49566865
1	0.24992431	1.65117323	2.56957741
1	-1.26445792	0.74853164	2.82911571
1	-1.20366137	2.50521226	3.15855443
6	-0.66451692	3.37487198	0.56038012
1	0.43014745	3.34472340	0.62247774
1	-1.02283025	4.18599443	1.20922166
1	-0.95897104	3.60887293	-0.47232889
6	0.36547757	0.43330152	-0.23473252
8	1.43632734	1.05169478	0.40502740
6	2.52858050	0.39191129	-0.07132781
6	3.87372083	0.61415838	0.25729385
1	4.17667222	1.36708211	0.98285174
6	4.78609126	-0.20444761	-0.38770939
1	5.84949022	-0.08881182	-0.16909002
6	4.40250580	-1.22242417	-1.32497335
6	5.37621323	-2.04992687	-1.94103883
1	6.43023834	-1.89637393	-1.70105460
6	4.99658001	-3.04889913	-2.82584806
1	5.75474206	-3.68348052	-3.28693723
6	3.63205774	-3.26129443	-3.12196575
1	3.34529027	-4.06342245	-3.80337540
6	2.65139735	-2.46789570	-2.54030028
1	1.59436846	-2.64136835	-2.74284038
6	3.01924008	-1.43982050	-1.64686097
6	2.08506935	-0.57822895	-0.99129990
7	0.72350360	-0.51603512	-1.08322170
26	-0.64912336	-3.23165820	2.20456412
35	-0.47999527	-4.03908053	-0.03800063
35	-2.65848970	-1.93424736	2.38397812
35	1.20962612	-1.80523170	2.66707765
35	-0.70106564	-5.01595961	3.71832886

Cartesian coordinates of the $C_{22}H_{19}N_2O^+$ cation

6	-1.02310788	0.48933414	0.37484316
6	-1.35908628	1.65634851	1.30247232
6	-2.87347085	1.66858851	1.20250487
6	-3.81929832	2.49297765	1.80580973
1	-3.52196651	3.29589228	2.48221075
6	-5.17684292	2.27200827	1.52407139
1	-5.93200944	2.90803822	1.98668763
6	-5.57776359	1.24580848	0.65413376
1	-6.63760949	1.09586241	0.44777337
6	-4.63791358	0.40819024	0.04148612
1	-4.96352241	-0.38110050	-0.63513419
6	-3.29402126	0.64554653	0.34087581
7	-2.14476185	-0.04662734	-0.13300913
6	-2.22269615	-1.18679651	-1.05212747

1	-3.27213000	-1.46710898	-1.17325234
1	-1.64985573	-2.02854290	-0.64803933
1	-1.79018057	-0.91497542	-2.02337599
6	-0.89691962	1.37408320	2.75832518
1	0.19720611	1.33945927	2.82357083
1	-1.30950485	0.42856088	3.13555680
1	-1.25569552	2.18481031	3.40677581
6	-0.75440089	2.98721635	0.77758262
1	0.34106084	2.96742334	0.82674124
1	-1.11250765	3.81218990	1.40823618
1	-1.06422577	3.19027387	-0.25649835
6	0.28066333	0.01767607	0.06166330
8	1.35431361	0.65046423	0.68242145
6	2.45307282	0.00207153	0.19666494
6	3.79666196	0.25084721	0.50455717
1	4.10156280	1.02918403	1.20195901
6	4.71127090	-0.56813636	-0.14093504
1	5.77593113	-0.42748259	0.05519378
6	4.33134678	-1.60024787	-1.06338104
6	5.31371003	-2.40729475	-1.69196401
1	6.36728019	-2.23422439	-1.46542639
6	4.94324055	-3.40514443	-2.58302860
1	5.70765237	-4.02013100	-3.05905289
6	3.58133080	-3.63008064	-2.87754808
1	3.30428196	-4.41643088	-3.58074131
6	2.59157215	-2.85784945	-2.27982752
1	1.53874824	-3.02887092	-2.50620317
6	2.94752151	-1.84054253	-1.37045059
6	2.00803509	-0.99398103	-0.69949942
7	0.64302794	-0.95728696	-0.76262236